# The Use of Polycaprolactone-Chitosan Scaffolds Combined with Bone Marrow Stromal Cells for Repairing Calvarial Defects

**Vivek Mantala**

**A Thesis Submitted in Partial Fulfillment of the Requirements for the Degree of**

**Master of Science in Oral and Maxillofacial Surgery**

**Prince of Songkla University**

**2014**

| | |
|---|---|
| **Thesis Title** | The Use of Polycaprolactone-Chitosan Scaffolds Combined with Bone Marrow Stromal Cells for Repairing Calvarial Defects |
| **Author** | Mr. Vivek Mantala |
| **Major Program** | Oral and Maxillofacial Surgery |

---

**Major Advisor :**

…….....

(Asst. Prof. Dr. Nuttawut Thuaksuban)

**Co-advisor**

…….....

(Assoc. Prof. Pleumjit Boonyaphiphat)

**Examining Committee :**

……..Chairperson

(Assoc.Prof.Dr. Theeralaksna Suddhasthira)

……...

(Asst. Prof. Dr. Nuttawut Thuaksuban)

……...

(Assoc. Prof. Pleumjit Boonyaphiphat)

……

(Asst. Prof. Dr. Suttatip Kamolmatyakul)

The Graduate School, Prince of Songkla University, has approved this thesis as partial fulfillment of the requirements for the Master of Science Degree in Oral and Maxillofacial Surgery.

…….……..

(Assoc.Prof.Dr.Teerapol Srichana)

Dean of Graduate School

This is to certify that the work submitted is the result of the candidate's own investigations. Due acknowledgement has been made of any assistance received.

……...

(Asst. Prof. Dr. Nuttawut Thuaksuban)

Major advisor

……...

(Vivek Mantala)

Candidate

I hereby to certify that this work has not been accepted in substance for any degree, and is not being currently submitted in candidature for any degree.

……...

(Vivek Mantala)

Candidate

**ชื่อวิทยานิพนธ์** การใช้โครงร่างโพลีคาโปรแลคโตน-ไคโตซานร่วมกับเซลล์สร้างกระดูกเพื่อรักษารอยวิการของกะโหลกศีรษะ

**ชื่อผู้เขียน** วิเวก มานตาลา

**สาขาวิชา** ศัลยศาสตร์ช่องปากและแมกซิลโลเฟเชียล

**ปีการศึกษา** 2556

## บทคัดย่อ

การศึกษานี้เป็นการประเมินความสามารถในการสร้างกระดูกใหม่ในรอยวิการกะโหลกศีรษะกระต่าย ภายหลังจากใส่โครงร่างสามมิติที่มีส่วนผสมของโพลีคาร์โปรแลกโตนและไคโตซานในอัตราส่วน 80 ต่อ 20 ซึ่งผลิตโดยวิธีเมลท์สเตรทชิ่งและมัลติแลย์เดพโพซิชัน ร่วมกับเซลล์ไขกระดูกสตรอมาอัตมันจากไขกระดูกของกระต่าย

การทดลองใช้กระต่ายนิวซีแลนด์ไวท์จำนวน 15 ตัว ทำการผ่าตัดนำไขกระดูกจากกระดูกเชิงกรานของแต่ละตัวมาคัดแยกเซลล์ไขกระดูกสตรอมาในห้องปฏิบัติการ ทำการเพาะเลี้ยงเพื่อเพิ่มปริมาณและกระตุ้นให้เจริญเป็นเซลล์สร้างกระดูก จากนั้นใส่เซลล์ของสัตว์ทดลองแต่ละตัวจำนวน $1.5 \times 10^7$ เซลล์ ลงแยกเลี้ยงในโครงร่างดังกล่าว (กลุ่มทดลอง เอ) ทำการผ่าตัดสร้างรอยวิการขนาดเส้นผ่านศูนย์กลาง 11 มิลลิเมตรบนกะโหลกศีรษะของกระต่ายแต่ละตัวจำนวน 2 ตำแหน่ง จากนั้นสุ่มใส่โครงร่างกลุ่มทดลอง เอ 1 ตำแหน่ง และใส่โครงร่างเพียงอย่างเดียว (กลุ่มทดลอง บี) 1 ตำแหน่ง ที่ช่วงเวลาการศึกษาที่ 2, 4 และ 8 สัปดาห์หลังการผ่าตัด นำกระดูกกะโหลกของสัตว์ทดลองมาวัดปริมาณการสร้างกระดูกและหลอดเลือดใหม่ในรอยวิการ รวมถึงประเมินปฏิกิริยาของเนื้อเยื่อโดยรอบโครงร่างโดยใช้วิธีการถ่ายภาพรังสีส่วนตัดอาศัยคอมพิวเตอร์ระดับไมโครเมตร และวิธีการทางมิญชวิทยา (5 ตัวอย่าง ต่อกลุ่มทดลอง ต่อช่วงเวลา)

จากการวัดทางมิญชวิทยาพบว่ากลุ่มทดลอง เอ มีปริมาณการสร้างกระดูกใหม่เฉลี่ยมากกว่ากลุ่มทดลอง บี ในทุกช่วงเวลาการศึกษาอย่างมีนัยสำคัญทางสถิติ ($p < 0.05$) อย่างไรก็ตาม จากการวัดด้วยภาพรังสีส่วนตัดอาศัยคอมพิวเตอร์ระดับไมโครเมตรพบว่าปริมาณการสร้างกระดูกใหม่ของทั้งสองกลุ่มไม่มีความแตกต่างกัน ($p > 0.05$) การวัดการสร้างหลอดเลือดใหม่ทางมิญชวิทยาพบว่าปริมาณหลอดเลือดใหม่ของกลุ่มทดลอง เอ มีมากกว่ากลุ่มทดลอง บี ในทุกช่วงเวลาการศึกษาและพบความแตกต่างอย่างมีนัยสำคัญทางสถิติที่ช่วงเวลา 8 สัปดาห์ จึงกล่าวโดยสรุปได้ว่า การใช้โครงร่างสามมิติโพลีคาร์โปรแลกโตนและไคโตซานร่วมกับเซลล์ไขกระดูก

สตรอมา ไม่สามารถกระตุ้นการสร้างกระดูกใหม่ในรอยวิการได้มากกว่าการใช้โครงร่างเพียงอย่างเดียวแต่สามารถทำให้เกิดการสร้างหลอดเลือดใหม่ได้มากกว่า ซึ่งจะส่งผลดีต่อกระบวนการหายของเนื้อเยื่อในรอยวิการ

| | |
|---|---|
| **Thesis Title** | The Use of Polycaprolactone-Chitosan Scaffolds Combined with Bone Marrow Stromal Cells for Repairing Calvarial Defects |
| **Author** | Vivek Mantala |
| **Major Program** | Oral and Maxillofacial Surgery |
| **Academic Year** | 2013 |

## Abstract

Polycaprolactone-chitosan three-dimensional scaffolds containing 20% chitosan (PCL-20%CS) were successfully fabricated using the Melt Stretching and Multilayer Deposition (MSMD) technique. This study evaluated the ability to repair bone defects in rabbit models of those scaffolds combined with autogenous bone marrow stromal cells. The culture-expanded bone marrow stromal cells were harvested from each of fifteen New Zealand white rabbit's iliac crests. After stimulated to be differentiated osteoblasts, the cells of $1.5 \times 10^7$ were seeded on to each scaffold. For each rabbit, two calvarial defects of 11 mm in diameter were created and the autogenous cell-scaffold construct was implanted in one site (group A) while another site was performed with the scaffold alone (group B). At two, four and eight weeks thereafter, new bone regeneration and new vessel regeneration within the defects were assessed using histomorphometric and micro-computed tomography (μ-CT) analysis (n=5/group/time point). The histomorphometric analysis demonstrated that the average newly formed bone of group A was greater than that of group B at every time-point ($p < 0.05$). However, the μ-CT analysis indicated that the newly formed bone of both groups were not significantly different ($p > 0.05$). The mean vessel counts in group A were higher than that of group B in every time points and statistically difference was detected in week 8. In conclusion, the PCL-CS scaffolds combined with the autogenous bone forming cells did not enhance more bone regeneration when compared to the scaffolds alone. However, the combination could allow more vessel regeneration throughout their inner portions that can increase the tissue healing and survival of the grafted scaffolds.

**Acknowledgement**

Foremost, I offer my sincerest gratitude to my principal supervisor Asst. Prof. Dr. Nuttawut Thuaksuban and co-supervisor Assoc. Prof. Pleumjit Boonyaphiphat who have supported me throughout my thesis with their patience and knowledge. I attribute the level of my Master of Science in Oral and Maxillofacial Surgery degree to their encouragement and effort and without them this thesis, too, would not have been completed or written. I am grateful to all the Oral and Maxillofacial Surgery Department staffs who promoted a welcoming academic and social environment.

I would like to acknowledge Mr. Jakchai Jantaramano and Ms. Supaporn Sangkert for their assistance in all of animal surgical procedures. I also thank all the staffs at the Animal house, Faculty of Sciences, Prince of Songkla University for providing and caring the animals throughout the study period. I also would like to acknowledge Mr. Kemarajt Kemavongse and all the staff at the Research Center, Faculty of Dentistry, Prince of Songkla University, for providing the proper setting and introduction to the laboratory tools application. I would also like to thank all the staff at the department of Pathology, Faculty of Medicine, Prince of Songkla University, who kindly helped in preparing the histological specimens. Many thanks are extended to all my fellow postgraduate students especially Ms. Suthasinee Sa –Nguanchuea, who as a good friend, with her kind support and guidance on the statistical software and life in Songkhla. I would like to thank my fellow, Ms. Chonticha Chookiatsiri, who kindly took care of my clinical works whenever I needed help.

Last, but by no means least, I thank my parents for love, encouragement and supporting with their best wishes throughout all my studies at the university. My studies and research would not have been possible without them.

Vivek Mantala

# Contents

**Contents (Continued)**

## List of Tables

## List of Figures

## List of Figures (Continued)

## List of Abbreviations and Symbols

| | | |
|---|---|---|
| AF | = | Area fraction |
| CS | = | Chitosan |
| *et al* | = | And others |
| Fig. | = | Figure |
| h | = | Hour |
| HB | = | Host bone |
| H&E | = | Hematoxylin-eosin |
| kg | = | Kilogram |
| kVp | = | Kilovoltage peak |
| mA | = | Milliampere |
| NB | = | Newly formed bone |
| NC | = | Necrotic tissue |
| PCL | = | Poly-caprolactone |
| ROI | = | Region of interest |
| SC | = | Scaffolds |
| TCP | = | Tricalcium phosphate |
| TE | = | Tissue engineering |
| VF | = | Volume fraction |
| W | = | Watt |
| µ-CT | = | Micro computed tomography |
| $\mu m^3$ | = | Cubic micrometer |
| µm | = | Micrometer |

# Chapter 1

## Introduction

Bone defect repairing is one of the most important tasks in oral and maxillofacial surgery[1]. As bone fails to self-regenerate in critical size defects, bone grafting is needed[2, 3]. Bone graft materials can be categorized by their origin into four groups: autografts, allografts, xenografts and synthetic grafts[4]. In addition, characteristics of those materials can be classified into three groups including osteogenesis, osteoinduction and osteoconduction[5]. At the present, only autografts elicit osteogenesis properties[4-6] and it has been considered the gold standard for bone grafting material[7-9]. Nonetheless, the disadvantages of the autografts are requiring more surgical sites that increases morbidity and limited amount of bone[5, 9-11]. Regarding these drawbacks, allografts and xenografts are more widely used. Their osteoconductive properties have been accepted with good clinical results[12]. However, the risk of disease transmission from those materials has been reported as about 1 in 1.6 million[1, 4] and an immunological reaction is also a possibility for caution[6]. Moreover, procedures to prepare the grafts also demolish the strength and osteoinductive proteins[10, 12]. Alloplasts are grafting materials that not produced from living donors. They can be defined as a synthetic, inorganic or biologically organic and can be implanted for repairing bone defects instead of human bone graft [7]. Ideally, the essential properties for the alloplastic materials include bioactivity, biocompatibility, minimal inflammatory responses and similar physical properties to bone[6, 7, 13, 14]. These types of graft materials e.g. bioactive glasses, calcium sulfate, calcium phosphates, tricalcium phosphate (TCP), hydroxyapatite (HA) and polymers has become more popular in the maxillofacial reconstruction branch and they often provide good clinical outcomes [6, 7, 15]. Nowadays, the trend of several studies is to develop optimum bone regenerative materials focusing on synthetic bioactive materials used for scaffolding.

The composite scaffolding is a combination of two or more biomaterials aiming to produce synergistic properties. Poly ε-caprolactone (PCL) and chitosan (CS) are very popular biomaterials used for that purpose due to their unique properties. PCL is approved by the Food and Drug Administration (FDA) as a medical and drug delivery device and it has been extensively supported by several in vitro and in vivo studies[16-20]. PCL is degraded by a hydrolytic mechanism under physiological conditions and it produces a less acidic environment when compared to other polyesters[16, 21]. However, since it possesses hydrophobic properties, PCL normally takes more than 24 months for complete degrading[21], which is not commensurate with the bone remodeling. CS is the second most abundant natural polysaccharide obtained by alkaline deacetylation of chitin. CS has been widely used as a biomaterial for many years due to its biocompatibility and bioactivity. It is known that the bioactivity of CS is mainly due to its cationic amine groups which can interact with anionic glycosaminoglycans (GAGs), proteoglycans and other negatively charged molecules on the surfaces of cells[22-25]. In addition, the major effects of chitosan on accelerating wound healing and promoting growth and differentiation of osteoblast cells have been reported over the last several years[26-31].

Recently, Thuaksuban *et al*[32] developed the novel technique of Melt Stretching and Multilayer Deposition (MSMD) specifically for fabricating the PCL-CS three-dimensional (3-D) scaffolds. MSMD processing is a melt blending technique without any porogens and solvents, therefore it is considered clean. The scaffolds including pure PCL scaffolds and PCL-CS scaffolds containing 10% and 20% CS by weight were successfully fabricated using this technique[32]. The PCL-CS scaffolds were specifically designed to be an appropriate interconnecting pore system for enhancing osteogenesis. A microgroove pattern, typically found on the surfaces of those scaffolds has proved to support attachment of osteoblasts[32]. In addition, the mechanical properties of the scaffolds are suitable for withstanding forces occurring in real circumstances of the reconstruction in the oral and maxillofacial region[33]. According to our previous study[32], the PCL-20%CS scaffolds achieved the most superior results for supporting osteoblast proliferation, followed by PCL-10%CS scaffolds and pure PCL scaffolds, respectively. The following experiments also indicated that the cells cultured on the PCL-20%CS scaffolds could produce more mineralized matrixes than those with other proportions. In addition, the

ability to repair bone defects of the PCL-20%CS was assessed and compared with commercial PCL- tricalcium phosphate (TCP) scaffolds. However, the result showed that the ability of both types of scaffolds could only gain small amount of new bone regeneration in rabbit models that is insufficient for reconstructing the larger bone defects. Therefore, finding ways to enhance that efficacy of scaffolds is still challenging. Regarding the fundamental aspects of bone regeneration, which include osteoconduction, osteoinduction and osteogenesis, it seems the later aspect is the most effective way of enhancing new bone formation. The strategy of combining biodegradable scaffolds with bone forming cells is a non-invasive technique and very practical for clinical applications.

## Review of Literature

### Bone tissue engineering

Tissue engineering (TE) is a multidisciplinary subject that attempts to restore the function of diseased or damaged tissues through the use of cells, biomaterials and biologically active molecules[1, 11, 14, 34]. The three basic components or the so-called "Tissue Engineering Triad" consist of cells, signaling molecules (or growth factors) and scaffolds[11, 34] (Fig. 1). The major aim of TE is to rebuild body structures to replace missing functions of the critical organs which lack the natural capacity for self-repair such as cardiac tissue, bone and cartilage[14, 35]. Currently, the therapeutic strategies for bone TE range from implantation of bone-like tissue which produced in vitro and in situ bone tissue regeneration[1, 13].

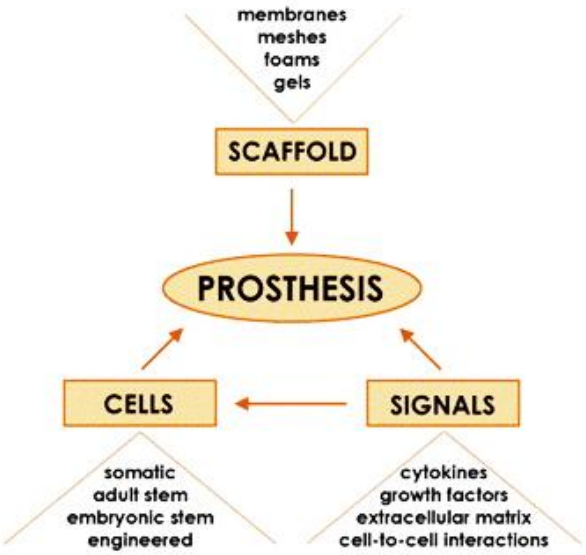


**Fig. 1** Tissue engineering triad consists of cells and signaling molecules (growth factors) that provide desired phenotypes and behavior of the cells. Scaffold acts as a template for tissue formation by allowing the cells to migrate, adhere, and develop organ tissue[34].

The first TE report was done by Howard Green in late 1970. Colonies of epidermal keratinocytes were grown into sheets of epithelium. The components were successfully transferred to dermal wounds in a rodent study[36]. The current approach in TE has shifted from cell-based to scaffold-based strategies as well as the use of osteogenic growth factors and genetic engineering[11] (Fig. 2).

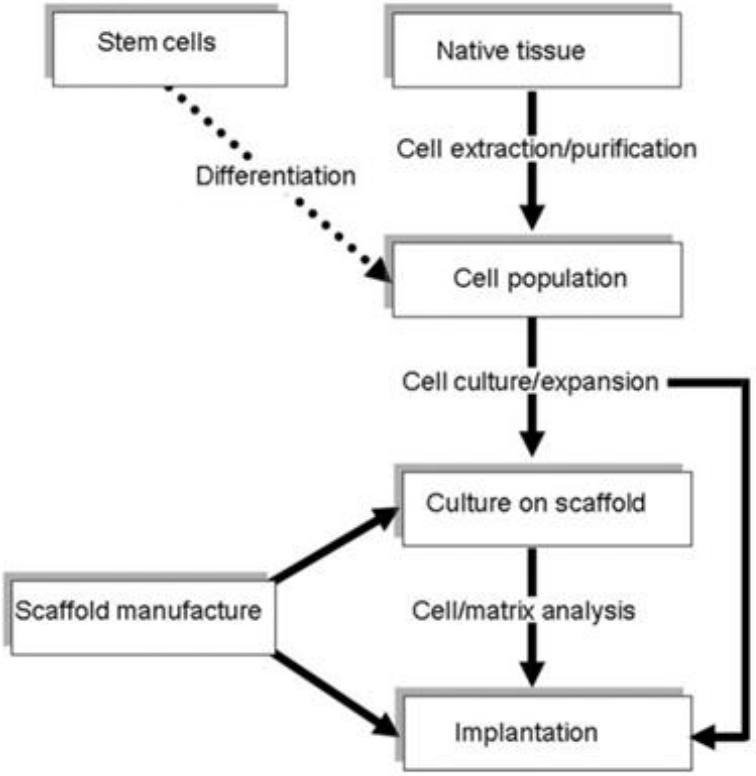


**Fig. 2** This schematic diagram demonstrates the scaffold-based tissue engineering theory[36]. Cells derived from tissue or stem cell sources can be used to combine with the scaffold. The cell- scaffold combinations are expected to have an ability to form tissues after implantation.

### Scaffold

The scaffolds should act as a framework for supporting growth and functions of desired tissue as well as maintaining shape and contour of the organ[37]. Two features of the scaffolds that influence cellular responses are 3-D architecture and the physico-chemical properties of their surfaces[1, 11]. The scaffolds should have the 3-D structures with highly porous and interconnected pore network for cell in-growth and transporting nutrients and metabolic waste. The macropore-size of 300-500 μm has been proven to enhance rates of nutrient transport as well as support growth of osteoblast cells[38]. The physico-chemical properties are a consequence of the material composition of the scaffolds[1, 13]. The major types of biomaterials can be divided into three categories of metals, ceramics and polymers. Metals yield the least satisfaction in bone tissue engineering because they are not biodegradable. Ceramics, like HA and TCP, give good results regarding bone regeneration, however, their major drawbacks are unpredictable degradation rate and low mechanical stability[39]. Up until the present, many approaches in bone TE have relied on synthetic biodegradable polymers, which are the regulatory approved biodegradable polymers such as polyglycolide (PGA), polylactides (PLLA, PDLA) and PCL, due to their tailor-made properties and processability.

## The materials

### Polycaprolactone

With FDA approval, PCL is widely used for fabricating bone regenerative scaffolds due to its biocompatibility and ease of fabrication[32, 40, 41]. PCL is a semi-crystalline aliphatic polyester (Fig. 3) with excellent processability due to a low melting temperature at 60$^{o}$C [32]. It has good mechanical properties and also acts as an osteoconductive material for bone cells[42, 43]. The drawbacks of PCL are its lack of osteoinductivity and slow rate of degradation[37, 40, 41]. To improve the osteoinductivity of PCL, attempts have been made to combine several osteoinductive materials with PCL-based scaffolds such as TCP[18, 37, 43], CS[32, 40, 41, 44],

Resveratrol[45], Simvastatin[46], and bone morphogenetic proteins (BMPs)[47]. Moreover, to gain the osteogenesis property, bone marrow derived stem cells are also used to combine with the scaffolds[48, 49].

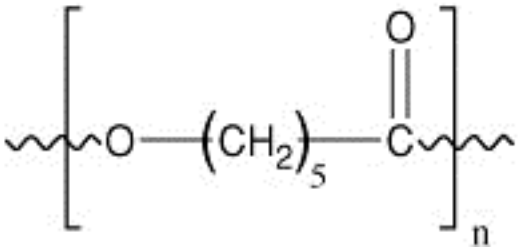


**Fig. 3** The chemical structure of PCL[50]

**Chitosan**

Chitosan is an aminopolysaccharide (poly-1,4-D-glucosamine) derived from an alkaline decetylation of chitin (Fig. 4). It has superior tissue biocompatibility due to its structure being similar to glycosaminoglycan in an extracellular matrix[26, 51]. Moreover, it has been proven to demonstrate properties needed for bone tissue engineering which include having biodegradability, a porous structure, suitability for cell ingrowth, osteoconduction, and an intrinsic antibacterial nature[32, 51]. CS has been widely applied in TE with various geometries and forms including films, fibers, beads and sponges[32, 40, 41, 44]. However, a major disadvantage of CS is poor physical property of being brittle at the dried stage[27].

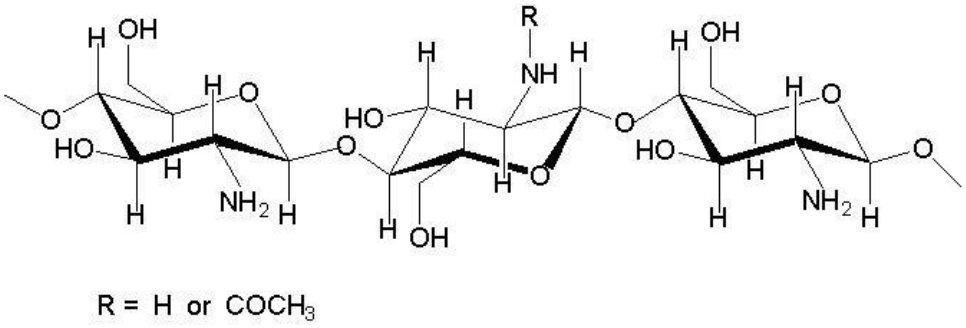


**Fig. 4** The chemical structure of Chitosan[52]

**Melt Stretching and Multilayer Deposition technique**

Thuaksuban *et al*[32] developed a MSMD technique of scaffolding using a melt-based processing. The technique utilizes the basic facilities of being practical, economical and suitable for industrial application. The concept of this technique is shown in Fig. 5. The MSMD PCL-CS scaffolds were the combination of a PCL matrix and CS filler using the melt blending[32]. Those scaffolds were hypothesized to improve the degradation and to enhance activities of bone cells. There were three ratios of the PCL and CS the were enrolled for the in vitro experiments including pure PCL (0 wt % CS), PCL-10%CS (10 wt % CS) and PCL-20%CS (20 wt % CS). Their architecture, degradation behavior and biomechanical properties as well as responses of the osteoblasts were assessed[32, 33](Fig. 6-8). Among the ratios, PCL-20%CS yielded the best result of supporting growth and differentiation of the osteoblasts.

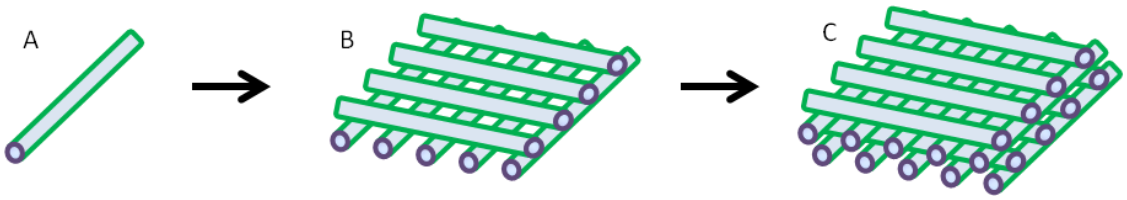


**Fig. 5** The concept of the MSMD technique to fabricate the 3-D scaffold is demonstrated. Firstly, the PCL-CS monofilaments are fabricated by melting and stretching, and reserved for constructing a monolayer scaffold (A). The monolayer scaffold is fabricated by aligning the filaments in a grid pattern with an average gap area of 500 μm (B). The 3-D scaffold is fabricated by depositing the monolayer scaffolds into multi-layers (C). Concerning this, the regularity of the interconnecting structure and pore size is controllable.

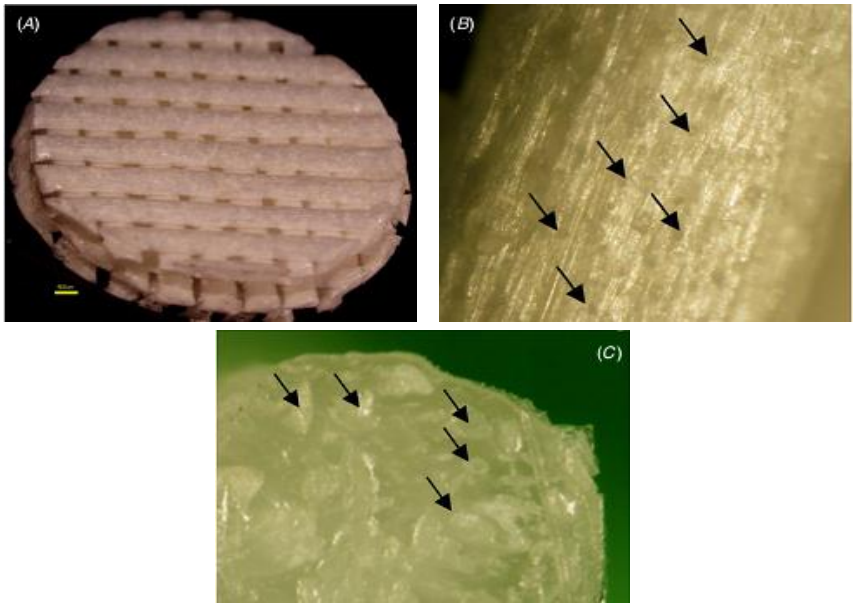


**Fig. 6** Stereomicroscope pictures of the PCL-CS scaffolds (A, scale bar = 500 μm). The PCL-CS filaments are opaque and small particles of CS are seen throughout the surface (B and C; arrows).

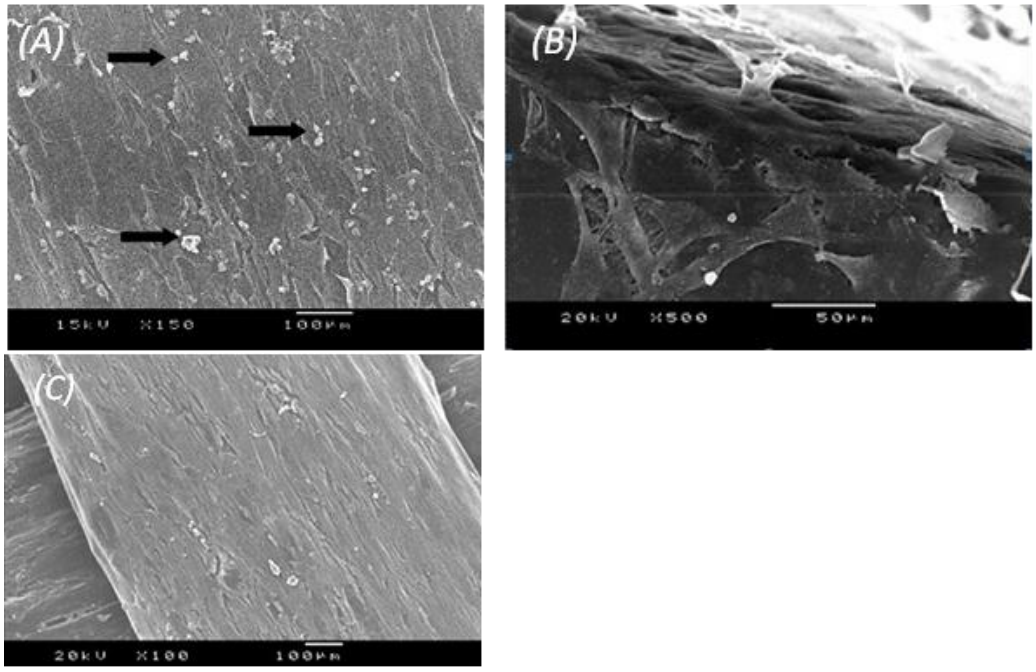


**Fig. 7** Scanning electron microscope (SEM) images demonstrate that osteoblast cells can grow in multilayers on the surface of PCL-20%CS scaffold. The mineralized nodules (arrows) indicate late differentiation of the cells on culture-day 7 (A). The picture at the edge of the scaffold's filament shows three-dimensional growth of the cells on culture-day 14 (B). A thick mineralized extracellular matrix covering all surfaces of the PCL-20%CS scaffold was found on culture-day 21(C).

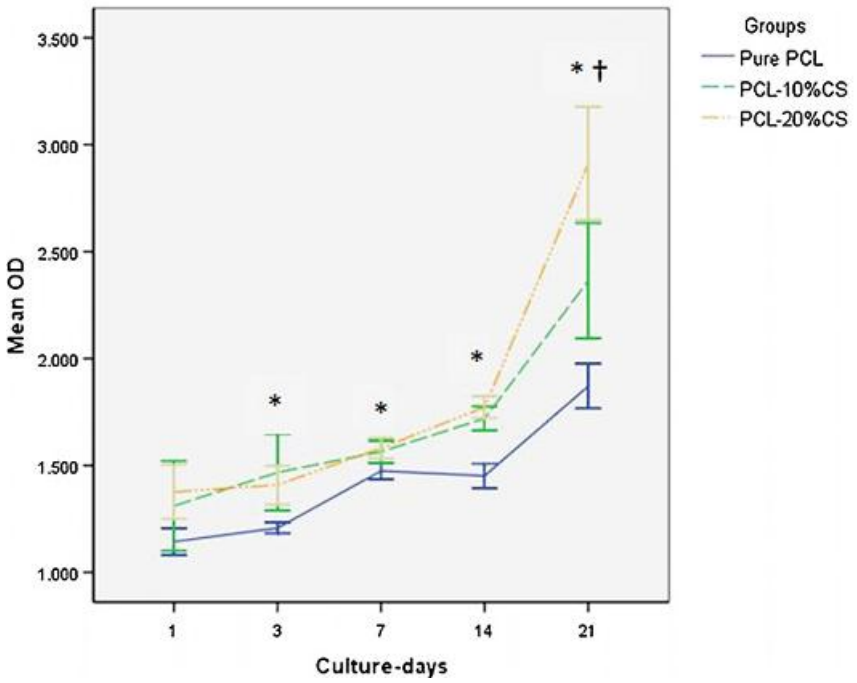


**Fig. 8** The graph demonstrates proliferation of the osteoblasts on the MSMD scaffolds over 21 days. At each time point after culture-day 1, the cell proliferation in the PCL-10%CS and PCL-20%CS groups was significantly higher than that in pure PCL group (* $P<0.05$). On culture-day 21, the cell proliferation in the PCL-20%CS group was significantly higher than the other groups († $p<0.05$).

Our other study (pending publication) aimed to assess efficacy of the PCL- 20% CS scaffolds for repairing rabbits' calvarial defects over 8 weeks of implantation in comparison with that of commercial PCL- 20%TCP scaffolds (Osteopore™, Singapore). The result indicated that the scaffolds of both groups could only gain a small amount of new bone at an average of 18.33 % and 20.20% of the defect size respectively (Fig. 9).

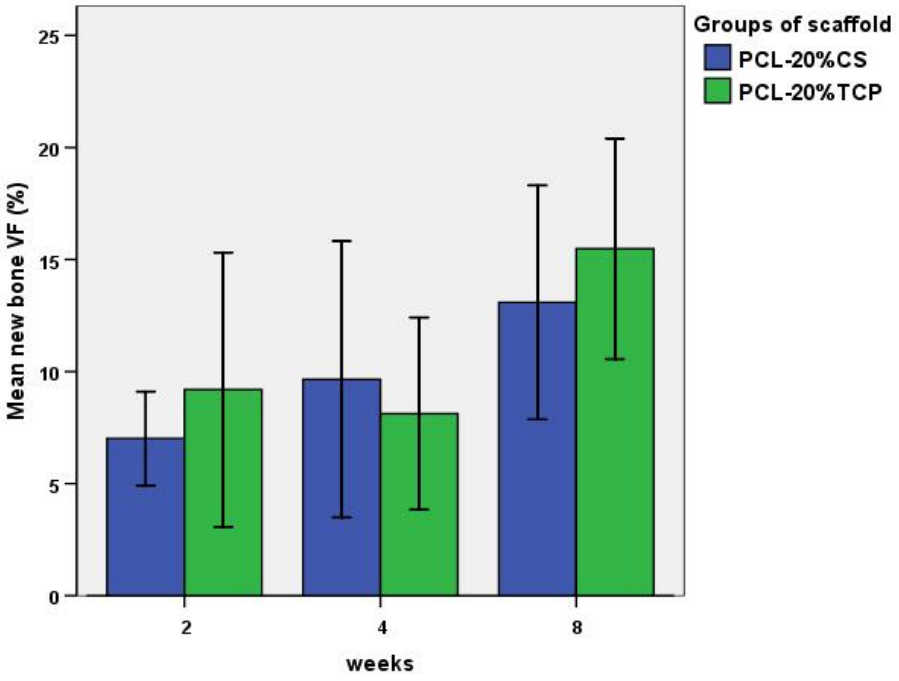


**Fig. 9** The graph shows the mean new bone volume fraction (VF) enhanced by PCL-20%CS and PCL-20%TCP scaffolds. Over 8 weeks, the amount of new bone of the two groups was not statistically different.

**The use of cells for bone TE**

Recently, bone TE has attracted awareness with the concept of regenerating bone tissue by using composites of osteoprogenitor cells and scaffolds. The engineered tissue fabricated in vitro involving combinations of cells and/or scaffold matrices would have ability to form tissue within the body upon transplantation. However, replacement of the tissue with autologous cells is an ideal situation from an immunological standpoint[36]. The cells from the autologous sources involve removal of tissue from the individual host, in vitro isolation and expansion for increasing amount of specific cells before re-implanting them to target sites. Regarding the types of the cells, stem cells play a key role in modern bone TE because of two essential properties including the capability of self-renewal and the ability to differentiate into diverse cell lineages under different conditions[36, 53, 54]. Stem cells are classified as embryonic stem cell, induced pluripotent stem cell and adult stem cell[55]. Adult stem cells are found in many human organs such as from bone marrow, adipose tissue and the umbilical cord. The mesenchymal stem cell (MSCs) is derived from bone marrow stroma and it is believed to be a multipotent stem cell (Fig. 10). The bone marrow derived mesenchymal stem cell has a high efficacy for using in bone TE, therefore, this cell type is very popular for many recent studies[49, 56]. However, the terms bone marrow derived mesenchymal stem cells and bone marrow derived stromal cells (BMSCs) are used interchangeably but indeed the majority of the cells in bone marrow stromal are not true stem cells[57, 58]. In general, MSCs in bone marrow stromal is relatively low as 0.01% to 0.001%[59-61] and their differentiation potential during culture is unstable[58]. Therefore, an efficient method of isolation and expansion is required. BMSCs are more suitable for bone TE than cells from other origins due to the following characteristics. Firstly, those cells have a high differentiate potential into multi-lineage e.g. osteogenic, chondrogenic and adipogenic lineage[61]. Secondly, it is easy to harvest them from a patient's donor sites such as bone marrow aspiration[60, 61]. Moreover, they have an immunosuppressive property, which can be modified to utilize from an allogenic source[62]. It is known that osteogenic differentiation of cultured BMSCs can be chemically induced by the addition of dexamethasone, ascorbic acid and beta glycerol phosphates[63, 64]. Among those substances, dexamethasone plays a crucial role in the

osteo-induction of the cell[65]. Other substances like basic fibroblast growth factors (bFGF) have been reported to affect and maintain the osteogenic ability of BMSCs'[66].

Several publications support the use of BMSCs combined with scaffolds. Schantz *et al* [67] seeded the culture expanded mesenchymal progenitor cells and osteoblasts from bone marrow into PCL 3-D scaffolds and implanted them into rabbit's calvarial critical-sized defects. After 3 months, the amount of calcification of the cell-seeded constructs was about 60% more than unseeded scaffolds. Zhou *et al* [49] combined cultured multilayered porcine bone marrow stromal cell sheets with PCL–calcium phosphate (CaP) scaffolds and transplanted the constructs under the skin of nude rats over 12 weeks. The results showed that neo-cortical and cancellous bone formed within the constructs increased up to 40% of the bone volume. Shao *et al* [68] seeded allogenic bone marrow-derived mesenchymal cells into pure PCL scaffolds combined with fibrin glue and implanted the constructs into the femoral condylar defects of rabbits. The results indicated that mature trabecular bone regularly formed in the scaffolds after 3 months post-implantation.

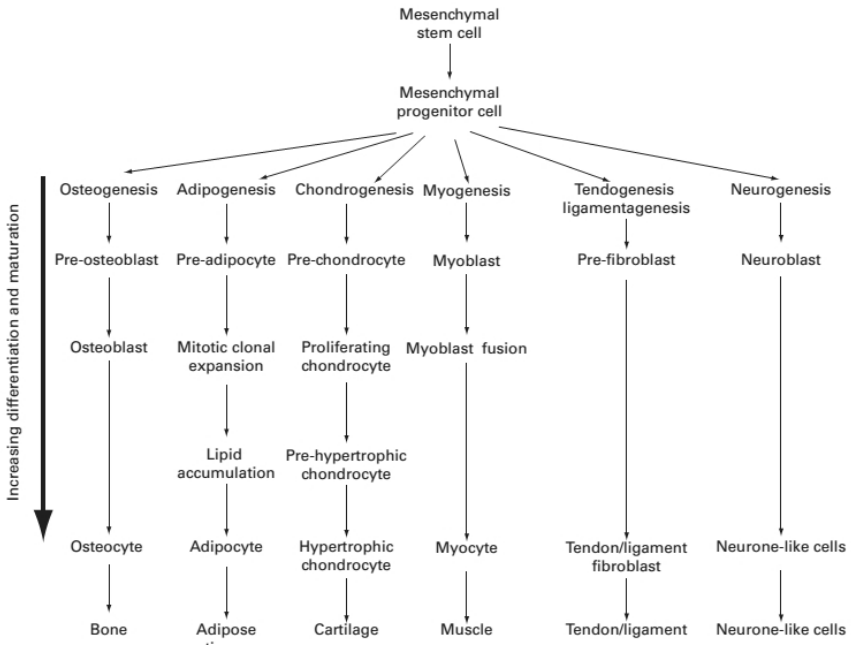


**Fig. 10** Diagram showing the multi-differentiation potential of mesenchymal stem cells[62].

Good cell-to-cell contact and distribution of the cells throughout scaffolds are the important factors for appropriate seeding procedures. In addition, seeding method and density of the cells have to be considered. In principle, the cell seeding methods can be classified into 3 categories: static seeding, dynamic seeding and magnetic seeding[36, 69]. The static seeding refers to an addition of cell suspension onto scaffolds like the soaking system[70] and pipette system[56] (Fig. 11). This technique is the simplest and most frequently used. However, this method is associated with a low seeding efficiency of approximately 10-25%[71]. Dynamic cell seeding is a procedure usually performed with bioreactor systems; for example, vacuum seeding using pressure differentials[72](Fig. 12). This technique yields higher seeding potential than static seeding, which ranges from 38 to 90%[60]. Magnetic cell seeding involves using a magnetic force to attract magnetic nanoparticles attached to desired cells or protein. It is a very effective method, but residual magnetic particles may be found in the organs and their adverse effects on tissues need further evaluation[69].

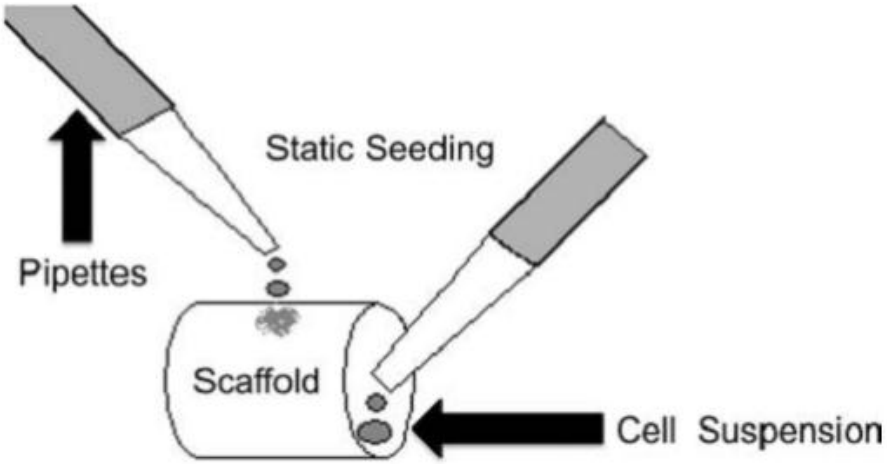


**Fig. 11** Static seeding[69]. Cell suspension is pipetted directly into the lumen of the scaffold or onto the outside of the scaffold.

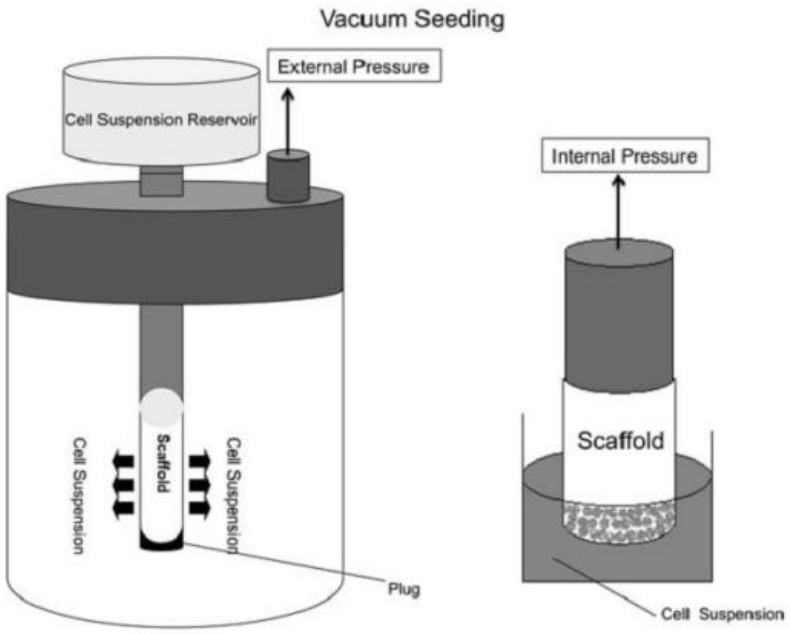


**Fig. 12** Vacuum/pressure seeding[69]. A cell suspension is forced through a scaffold by either internal pressure or external vacuum pressure. As cells travel through the scaffold, they become lodged in the pores.

**Hypothesis**

This study hypothesized that by combining autogenous BMSCs to the MSMD PCL-20%CS scaffolds, it would enhance more new bone regeneration than that resulting from the scaffolds alone.

**Objective**

The aim of this study was to assess new bone regeneration within the rabbit's calvarial defects enhanced by the PCL- 20% CS scaffolds combined with autogenous BMSCs compared to new bone regeneration from the scaffolds alone.

# Chapter 2

## Materials and Methods

### The scaffolds and study groups

The preparation protocol for the scaffold specimens is explained below. The PCL-20%CS scaffolds were fabricated using the MSMD technique according to the following protocols[32]. PCL pellets ($\overline{M}_n$ 80,000 PC, Sigma Aldrich, USA) and CS particles (CS middle-viscous, $\overline{M}_w$ $3 \times 10^5$–$5 \times 10^5$, 75–85% deacethylation, Fluka, Japan) were milled separately using a freezer-mill machine (SPEX Sample Prep LLC, USA). The CS micro-particles were prepared by sieving through a 75 micron-sieve (Retsch, Germany). The two materials were mixed together in the ratio of PCL: CS = 80:20 by weight and melted in a melting-extruding machine. The monofilaments were made by extruding the PCL-CS blend through the nozzle tip of the machine. After that, the filaments were stretched to decrease their diameter. The stretched filaments were used to form monolayer scaffolds by arranging and stamping them on to the poly-vinyl template. The pattern of the scaffolds was a grid pattern of filament lines at 90˚ to each other with average space area of 500 $\mu m^2$ between the lines. To prepare the multilayer (3-D) scaffolds as the testing specimens, the monolayer scaffolds were cut into round shapes of 11 mm in diameter using a round shaped poly-vinyl template. The 3-D scaffold was made by depositing three monolayer scaffolds in the pattern of $0^o/90^o$ for each layer and by repeated stamping (Fig. 13). All specimens were sterilized using ethylene oxide gas at 37˚C for 2h.

The study groups included group A: PCL- 20%CS scaffolds combined with autogenous BMSCs and group B: PCL- 20%CS scaffolds alone (n=5/group/time point, total n =15/group) (Table 1).

**Table 1** Study groups and animal used.

| Study groups | Number of defects | | Number of animals | |
|---|---|---|---|---|
| | Each time point | Total | Each time point | Total |
| **A** | 5 | 15 | 5 | 15 |
| **B** | 5 | 15 | | |

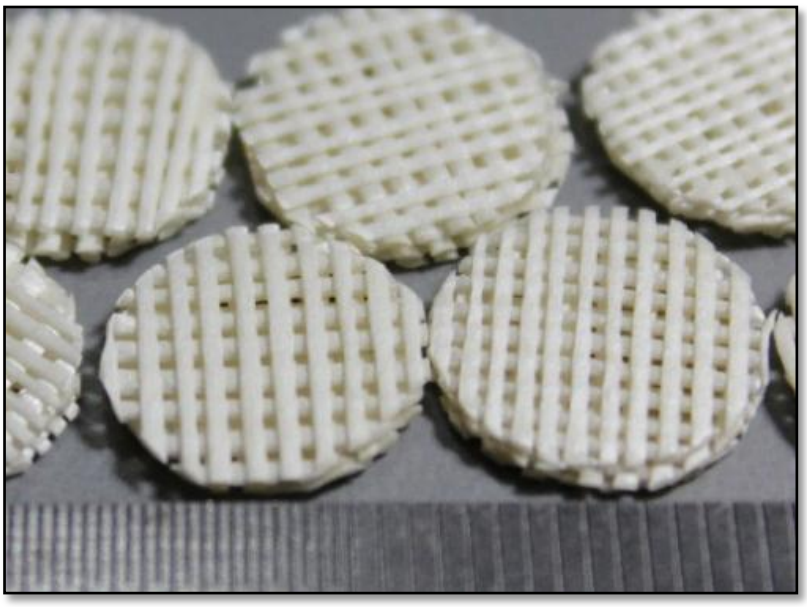

**Fig. 1** The picture of the PCL- 20%CS MSMD scaffolds prepared for the experiment.

**Bone marrow harvesting**

Fifteen adult male New Zealand white rabbits weighing 3.5 – 4 kg were included in the study. The in vivo experiment was approved by the experimental ethics committee of Prince of Songkla University. Each rabbit was anesthetized using an intravenous injection of 1 mg/kg diazepam and placed in the prone position. After injection of 2% lidocaine containing 1:100,000 epinephrine, approximately 25 $mm^3$ of cancellous bone was harvested from the iliac crest and placed into the transfer medium consisting of Dulbecco's Modified Eagle Medium

(DMEM, Gibco, Invitrogen, USA), 100 IU/ml of penicillin/streptomycin and 250μg/ml of Fungizone (Gibco, Invitrogen, USA) (Fig. 14). The surgical wound was closed with 4/0 absorbable sutures and the rabbits were received antibiotic prophylaxis with 0.1 mL/kg cephalexine for 3 days.

**Cell culture**

Bone marrow-derived stromal cells (BMSCs) were isolated from the cancellous bone particles by an explant technique under the following protocol. The periosteum and soft tissue was discarded and the bone was cut into small pieces. The bone pieces were transferred into 3.5 cm petri dishes and proliferation medium consisting of alpha Minimum Essential Medium (α-MEM, Gibco, Invitrogen, USA) supplemented with 10% Fetal Bovine Serum (Gibco, Invitrogen, USA), 100 IU/ml of penicillin/streptomycin and 250μg/ml of Fungizone (Gibco, Invitrogen, USA). The cells of each rabbit were cultured separately from each other to prevent any antigenic reaction. After 3 days, non-adherent cells were removed by replacing with fresh medium. The adherent cells were cultured in the medium until they exhibited the character of colony-forming fibroblast-like cells, before, sub-culturing was conducted for the first passage (P1) (Fig. 15). The P1-cells were cultured in the osteogenic medium to stimulate BMSCs to be well-differentiated osteoblasts. The osteogenic medium was prepared using the proliferation medium supplemented with 0.2 mM Ascorbic acid (Sigma, USA), 10 mM β-Glycerophosphate (Sigma, USA) and $10^{-8}$ M Dexamethasone (Sigma, USA)[64]. The osteoblastic characterization of those cells was assessed by the alkaline phosphatase (ALP) staining (Sigma, USA) and Alizarin Red staining (AR)(Sigma, USA)[66, 73](Fig. 16). The cells, which had the positive staining to ALP more than 60 percent were allowed to continue culturing. After 80% confluence, subculture was performed and the cells of P2-3 were used for the experiments.

**Preparing cell-scaffold constructs**

Prior to cell seeding, the sterilized PCL-20%CS scaffolds were immersed in fresh proliferation medium for 24h. Total BMSCs of 1.5 x $10^7$ cells explanted from each individual rabbit were seeded onto each PCL-20%CS scaffold using the static seeding method[69]. To ensure attachment of the cells throughout the scaffolds, seeding procedures were performed on each side of the scaffolds. For each scaffold, BMSCs of 7.5 x $10^6$ cells were seeded on one side of the scaffold and it was left in the incubator at 37˚C, 95%$CO_2$ for 3h to allow the cell to attach. Afterwards, the scaffold was flipped over and the same seeding procedure was repeated. The cell-scaffold constructs (group A) and the scaffolds without cells (group B) were cultivated in osteogenic medium for 3 days. Prior to the surgical implantation, the constructs were investigated using a light microscope (Olympus, Japan). Three constructs were additionally prepared to assess attachment and proliferation of the cells on the scaffold surfaces using a SEM (JSM5200, JEOL, Japan).

**Scanning electron microscope**

The constructs were removed from the culture plates and rinsed with phosphate buffered saline (PBS) and then fixed with 2.5% glutaraldehyde for 2 h. Next, they were dehydrated in an ethanol series of 30-100%. After that, a critical point drying procedure was performed. The constructs were coated with Gold-Palladium coating and observed via the SEM.

**Surgical implantation protocol**

The implantation procedure in the rabbits was performed under general anesthesia as previously described. For each rabbit, after sub-periosteal dissection, bi-cortical defects (11 mm in diameter) were created at both sides of its calvarium (Fig. 17 A). The scaffold of group A was randomly implanted in one side of the calvarium and the other side was implanted with that of group B (Fig. 17 B), and then the skin flap was closed with 4/0 absorbable sutures.

All rabbits were received antibiotic prophylaxis with 0.1 mL/kg cephalexine for 3 days. At the time points of 2, 4 and 8 weeks after the operation, the surgical wounds were clinically assessed. Healing and any complications of the surgical sites were descriptively recorded. After that, the rabbits were sacrificed with an overdose of intravenous pentobarbital sodium. Each calvarium was removed in one piece. The gross specimen was examined before fixing in 10% formalin. After 48 hrs, it was cut along the mid sagittal suture into 2 pieces of specimens using a cutting-gridding machine (Exakt, Germany). Micro-computed tomography ($\mu$-CT) analysis was conducted in all specimens before processing them for histomorphometric analysis.

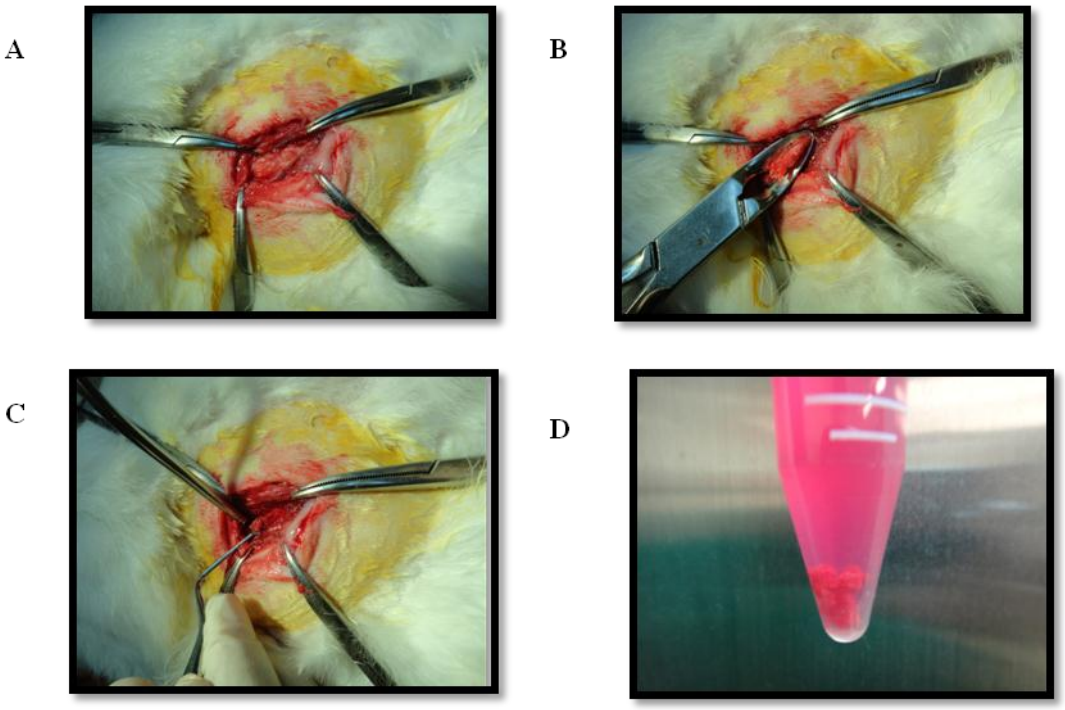


**Fig. 2** Bone marrow harvesting technique via supra-iliac crest approach (A). After periosteal dissection, the cortical bone along the crest was removed to expose the bone marrow (B). The bone marrow was harvested using a sharp curette (C). Harvested bone marrow was stored in the transfer medium (D).

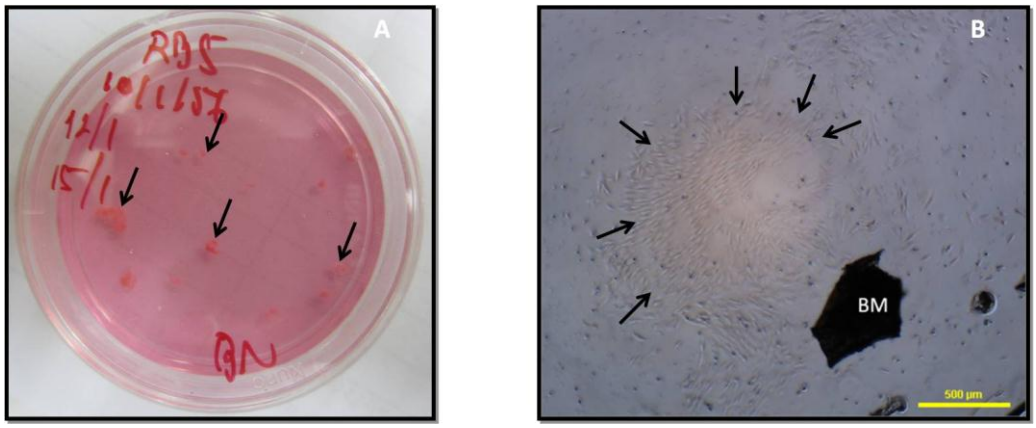


**Fig. 3** Primary explant culture of the bone marrow. Small pieces of the bone marrow (arrows) were cultured in the proliferation medium (A). The colony-forming fibroblast-like cells occurred after several days of culture (arrows) (B). Abbreviation: BM= bone marrow

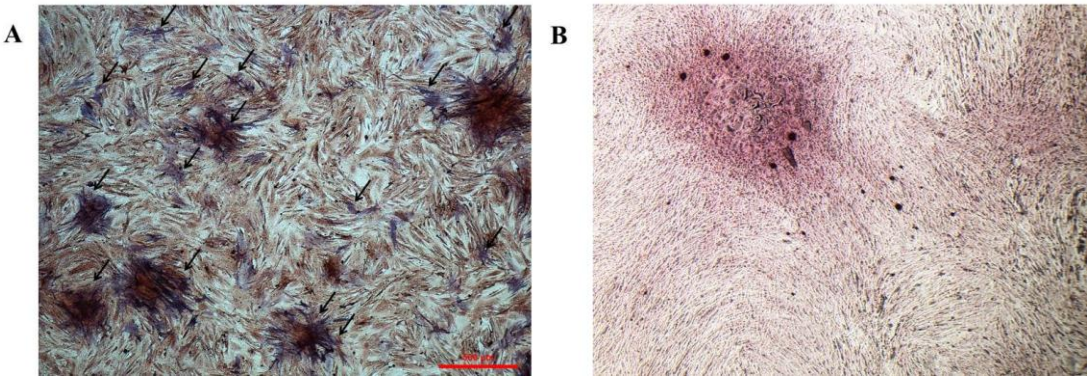


**Fig. 4** The formation of ALP-positive staining colonies (bluish- purple, arrows) (A) and AR-positive staining colonies (bluish-red) (B).

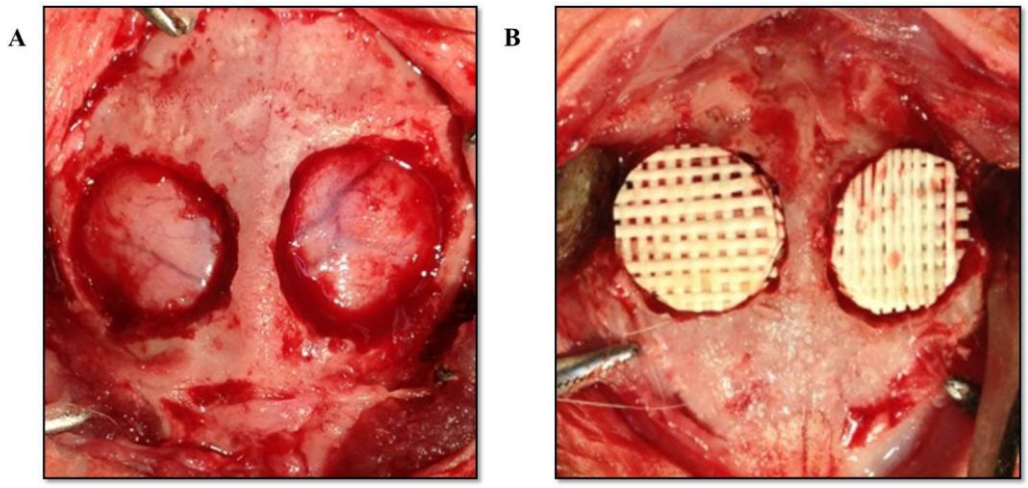


**Fig. 5** Two bi-cortical defects were created at both sides of the calvarium (A). The defects were implanted with the scaffolds; on the right is the scaffold of group A and the left one is the scaffold of group B (B).

**$\mu$-CT analysis**

The specimens of each time point (5 specimens/ group/ time point) were scanned using a $\mu$-CT ($\mu$CT 35, SCANCO Medical AG, Switzerland) in a direction parallel to the coronal aspect of the calvariums with a setting of 55 kVp, 72 µA and 4 W. The measuring parameter was the new bone volume fraction (VF) calculated by analysis software ($\mu$CT 35 Version 4.1, SCANCO Medical AG, Switzerland) using the following formula (Fig. 18A).

$$\textbf{New bone VF (\%)} = \frac{[\text{New bone volume}]}{\text{Defect volume}} \times 100$$

**Histologic processing and histomorphometric analysis**

The specimens were decalcified in formic acid and embedded in paraffin (5 specimens/ group/ time point). Serial 5-µm-thick sections were cut at the positions of 500 µm from the margin (Fig. 18A). The sections were stained with Haemotoxylin and Eosin (H&E) (3 sections/ specimen/ staining) and scanned using a slide-scanner (ScanScope, Aperio, USA) to be image files. The region of interest (ROI) was located between the rims of both sides of the defect including the newly formed bone, the surrounding tissue and the remaining scaffold (Fig. 18B). Microscopic features of the ROI were assessed descriptively. Area fractions (AF) of newly formed bone were calculated by the following formulas using analysis software (ImageScope, Aperio, USA). The defect area could be calculated by multiplying the average height of the defect rims (H) by the length of the defect (L). The area fractions were measured as percentages to prevent error due to shrinkage of the specimens.

$$\textbf{Defect area } (\mu m^2) = \frac{[H1+H2]}{2} \times L$$

$$\textbf{Newly formed bone AF (\%)} = \frac{[\text{Areas of new bone formation}]}{\text{Defect area}} \times 100$$

Those image files were also used for quantitatively assessing the levels of new vessel regeneration. In each histological section, customized five-grid template was used for creating the counting fields (Fig. 19). Assignment of the grids was carried out in the middle part of the scaffolds in the scanned images using the analysis software (ImageScope, Aperio, USA). With magnification of 10x, the vessels within the measuring fields were counted using strict criteria for the identification of endothelial cells lining and red blood cells. Blind counting was conducted by two persons; the experienced histopathologist and the main author. In cases where assessment differed, disagreements were resolved by consensus after joint review.

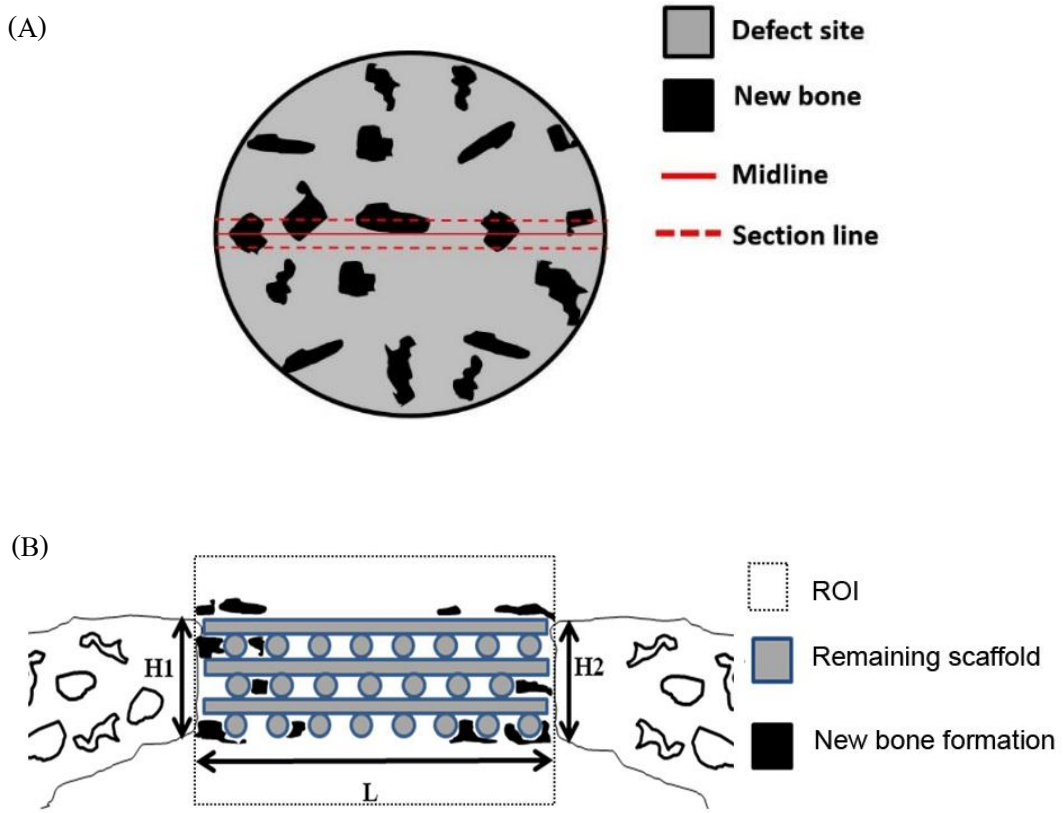


**Fig. 6** Schematic drawing for defining the defect site for the $\mu$-CT analysis and the section lines for the histomorphometric analysis (A) and schematic drawing for defining the ROI for the histomorphometric analysis (B).

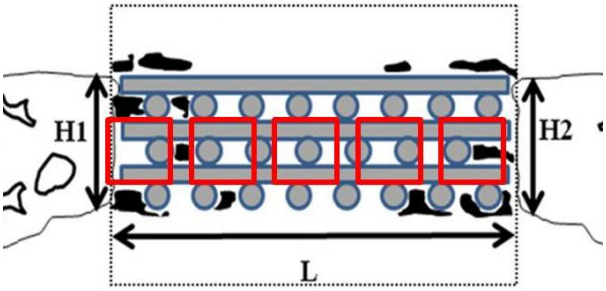


**Fig. 7** Schematic drawing for measuring new vessel regeneration. The template of customized square-shaped grids was superimposed on the histological image to create the measuring fields. All vessels within the fields were counted in duplicate.

**Statistical analysis**

The data was analyzed using statistical analysis software (SPSS, version 14.0, USA). The microscopic features of the scaffolds and the surrounding tissue were assessed descriptively. One-way Analysis of Variance (ANOVA) followed by Tukey HSD was applied to compare the differences of the measuring parameters among the healing intervals within each group. Dunnett's T3 test was performed when equal variances was not assumed. The paired *t*-test was applied to compare the differences of those parameters between the two groups for each time point. The level of statistical significance was set at a p value $< 0.05$.

# Chapter 3

## Results

### Characteristic of the BMSCs on the scaffolds

The SEM images prior to the surgical implantation demonstrated that BMSCs could attach well throughout the scaffold surfaces. In addition, the cells growing in multi-layers indicated their well proliferation (Fig. 20).

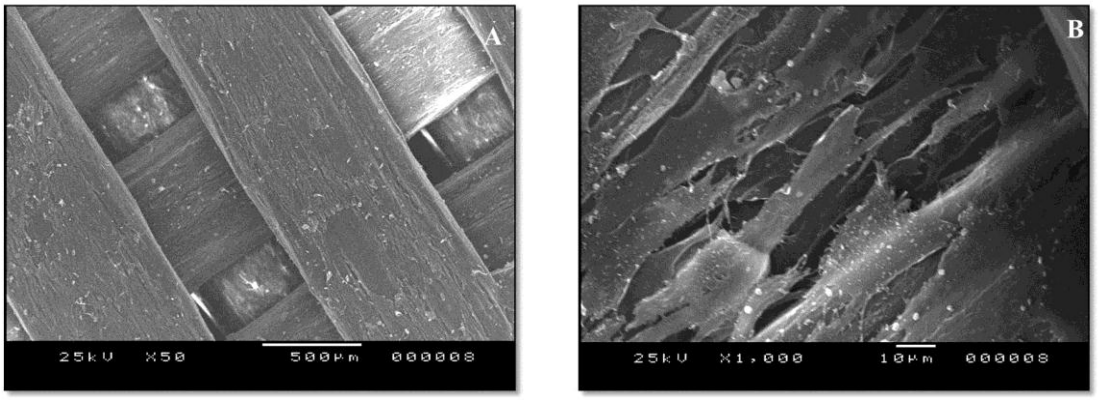


**Fig. 1** SEM images of day three post-seeding. The cells could attach and proliferate well throughout the scaffold surfaces (A). The magnified image shows spreading of the cytoplasmic processes of the cells and their growing in multi-layers (B).

### The experiment in animal models

All rabbits of both groups tolerated the operation well and they were healthy during the observation period. The surgical wounds clinically healed without complication.

**Gross specimens**

The gross specimens showed that healing of the implanted sites integrated well to the surrounding host bone. The surgical defects were covered with dense fibrous tissue without signs of foreign body reaction (Fig. 21).

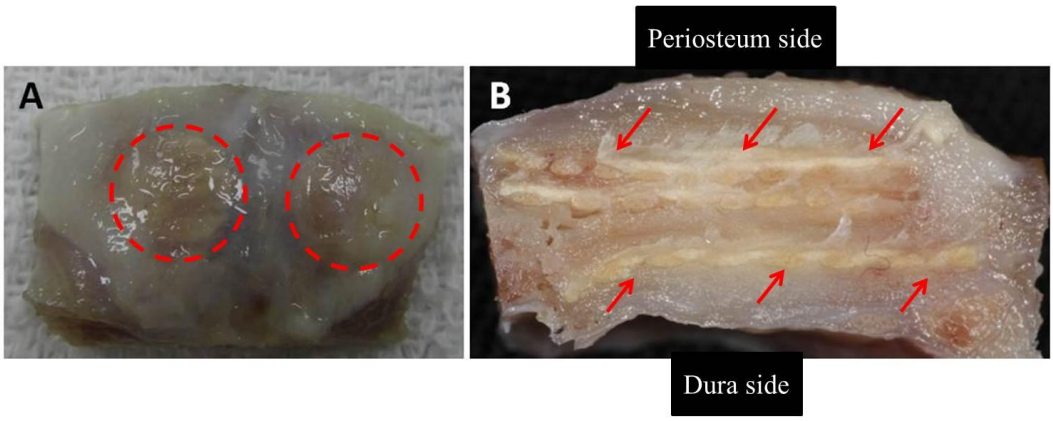


**Fig. 2** Gross specimens of the implanted sites (circular marks) at week 8. It was found that the scaffolds were embedded in place without clinical signs of inflammation (A). The implanted site was covered with periosteum and the scaffold (arrows) was surrounded with dense fibrous tissue (B).

**Histomorphometric analysis**

Histological features of the implanted areas are demonstrated in Fig. 22 – 24. During the histological preparation, the scaffolds of both groups were totally dissolved, hence the scaffold areas in the histologic images were seen as empty spaces. At week 2, the scaffolds of both groups were surrounded by dense fibrous tissue and neo-vascularization was clearly found throughout the inner parts of them. Chronic inflammatory cells, mainly eosinophils and histeocytes, were generally found infiltrating along the surfaces of the scaffolds of both groups. Some areas of necrotic tissue were also found in the deep parts of those scaffolds. By observation,

inflammatory cells and necrotic tissue were found to be more obvious in group B more than group A. New bone formation could be detected extending from the periphery of the defects but there was no bone formation observed within the scaffolds of both groups (Fig. 22). In week 4, an increase of neo-vascularization along with dense collagen connective tissue within the scaffolds was detected simultaneously with a remarked decrease in inflammatory response. In addition, the amount of new bone formation of both groups remarkably increased. The bone formation within the deep parts of the scaffolds was more obviously detected (Fig. 23). In week 8, most of that new bone of both groups matured and remodeled, hence it was difficult to distinguish between the newly formed bone and the host bone margins. Bone bridging characterization of the defects underneath the scaffolds of group A could be observed in some specimens, whilst it was not found in group B (Fig. 24). The newly formed bone AF is demonstrated in table 2 and Fig. 25. It was found that new bone formation of both groups increased with time. The new bone formation of group A was greater than that of group B at each time point and significant difference between them was found at weeks 2 and 4. The amounts of new vessels regenerating within the scaffolds are demonstrated in table 3 and Fig. 26. It was found that the scaffolds of group A allowed more vascular regeneration into their deep parts than those of group B at every time-point.

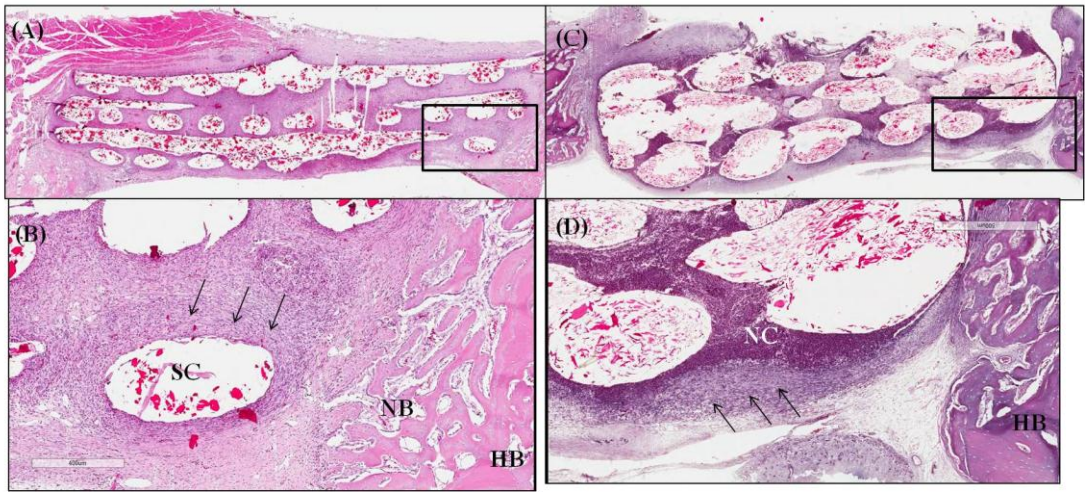


**Fig. 3** H&E stained sections of the implanted sites at week 2; group A: (A, B), group B: (C, D). The original section of group A shows that the outer regions of the scaffold are surrounded by fibrous tissue and newly formed bone regenerating from the periphery area (box) (A). The remnants of CS are seen as the red particles within the empty space. The 5X magnification image of the box shows that the scaffold surrounded by dense fibrovascular tissue. Chronic inflammatory cells are seen along the scaffold filaments (arrows) (B). The original section of group B shows that the outer regions of the scaffold are surrounded by dense fibrovascular tissue (C). Small amounts of new bone formation are also seen peripherally to the host bone area (box). The 5X magnification image of the box shows that the scaffold is surrounded by dense fibrovascular tissue (D). Thicker bands of chronic inflammatory cells are seen along the scaffold surfaces (arrows) and large areas of necrotic tissue are seen in the deep parts of the scaffold. Abbreviations: NB = newly formed bone, HB = host bone, SC = scaffolds, NC = necrotic tissue.

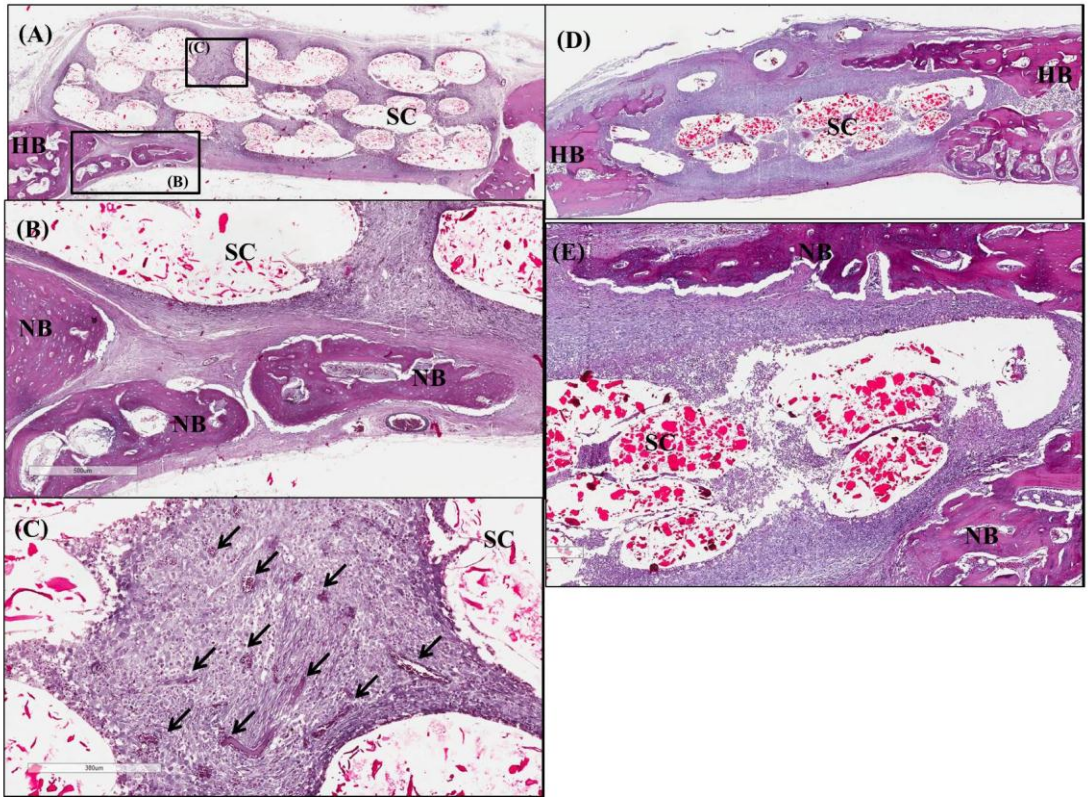


**Fig. 4** H &E stained sections of the implanted sites after four weeks; group A: (A - C), group B: (D, E). The original section of group A shows that inflammatory cells and necrotic tissue remarkably decrease, whilst increasing of new bone formation is seen along the inner surface of the scaffolds (A, box B). The 5X magnification image of box B shows woven patterns of the newly formed bone regenerating beneath the scaffold (B). The 10X magnification image of box C shows several newly formed vessels (arrows) in the deep part of the scaffold (C). The original section of group B shows that the scaffold is surrounded by dense fibrovascular tissue (D). New bone formation is also seen along the inner portion of the scaffold (box). The 5X magnification image of the box shows newly formed bone within the deep parts of the scaffolds (E). Less vascular formation is observed when compared with the scaffold of group A. Abbreviations: NB = newly formed bone, HB = host bone, SC = scaffolds.

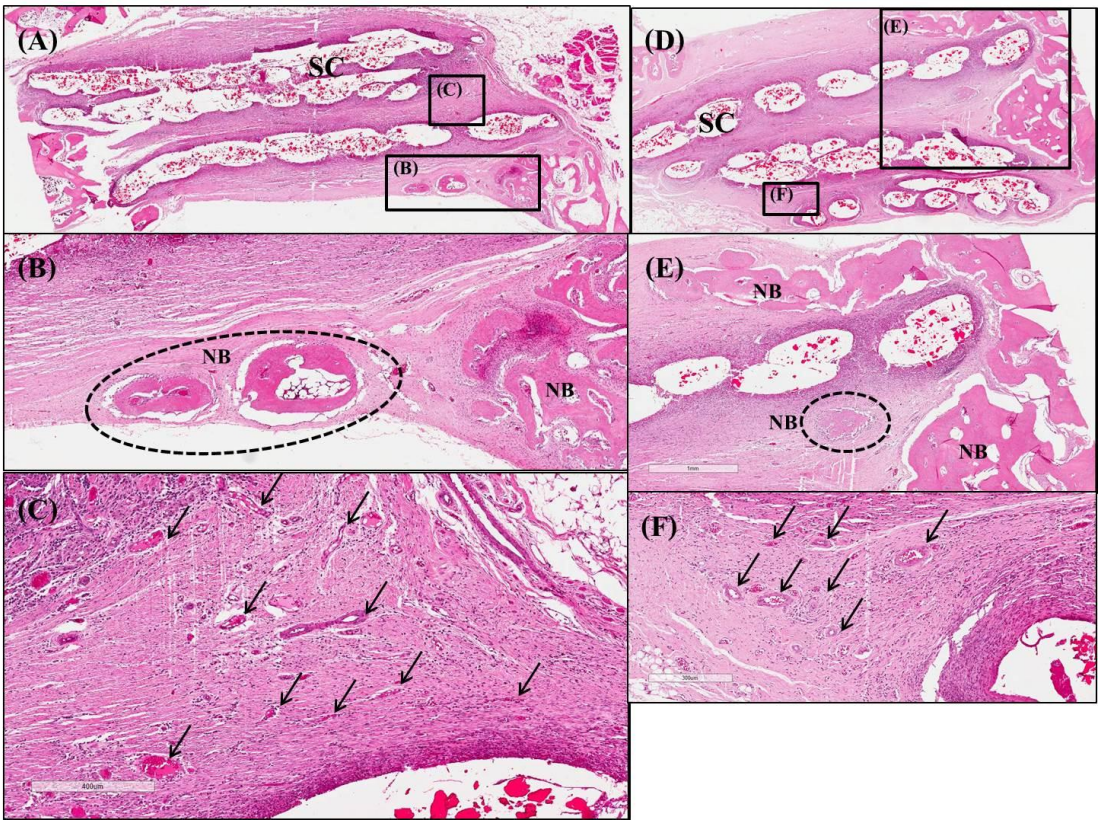


**Fig. 5** H &E stained sections of the implanted sites after eight weeks; group A: (A - C), group B: (D- F). New bone formation is generally found underneath the scaffold (A, box B). The 5X magnification image of box B (B). The 10X magnification image of box C demonstrates that high vascular regeneration (arrows) are observed within the deep parts of the scaffold (C). The original section of group B shows dense fibrous tissue within the scaffold (D). New bone formation is also seen. The 5X magnification image of box E shows maturing bone that tends to bridge the defect and new bone formation within the scaffold (circular marks) (E). The 10X magnification image of box F shows newly formed vessels (arrows) (F). Abbreviations: NB = newly formed bone, SC = scaffolds.

**Table 1** Histomorphometric data of the newly formed bone AF over the observation periods

| Study groups | Newly formed bone AF (%)(mean ± SD) | | |
|---|---|---|---|
| | 2 weeks | 4 weeks | 8 weeks |
| **Group A** | 3.768 ± 1.392 | 6.450 ± 1.631 | 7.090 ± 1.696 |
| **Group B** | 1.882 ± 0.784 | 3.707 ± 1.510 | 6.380 ± 1.184 |

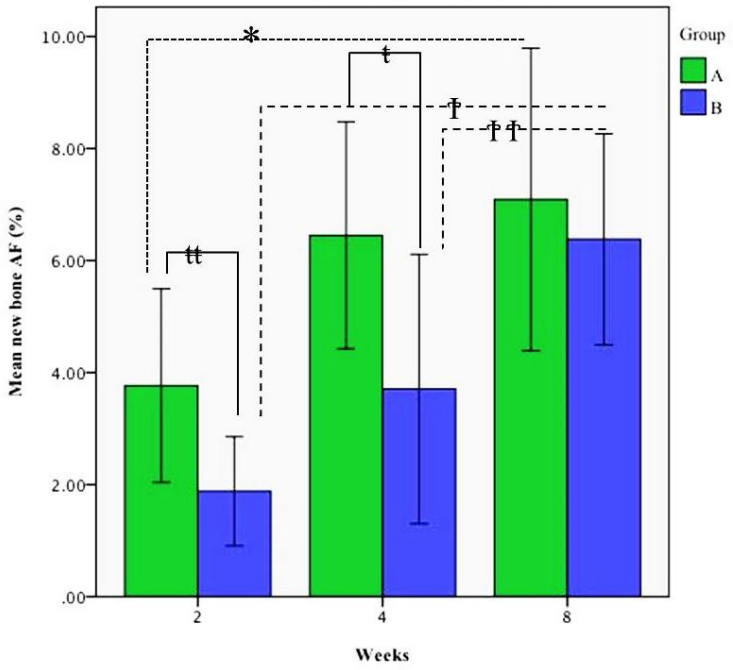


**Fig. 6** The graph of the newly formed bone AF. At weeks 2 and 4, new bone formation of group A is significantly greater than that of group B (ŧŧ: p = 0.030, ŧ: p = 0.036). In group A, newly formed bone AF at week 8 was significantly greater than the amount at week 2 (*: p = 0.024). In group B, newly formed bone AF at week 8 was significantly greater than the amount at weeks 2 and 4 (Ŧ: p = 0.00, ŦŦ: p = 0.022).

**Table 2** Histomorphometric data shows the numbers of new vessels within the scaffolds of both groups over the observation periods.

| Study groups | numbers of new vessels (mean ± SD) | | |
|---|---|---|---|
| | **2 weeks** | **4 weeks** | **8 weeks** |
| **Group A** | 21.800 ± 8.899 | 13.400 ± 12.779 | 43.750 ± 8.846 |
| **Group B** | 17.000 ± 12.903 | 4.250 ± 2.217 | 16.750 ± 7.274 |

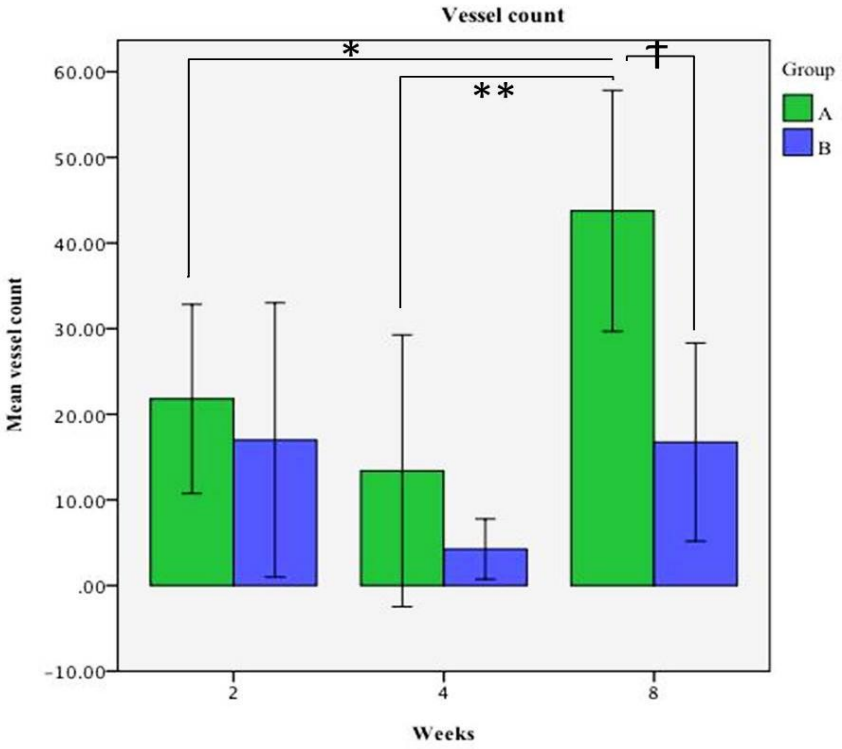


**Fig. 7** The graph of average vessel regeneration within the scaffolds. The mean vessel counts in group A were higher than those of group B at every time points but statistical difference was found only in week 8 (ANOVA, †: p =0.004). The mean vessel count of group A reached the maximum at week 8 and it was significantly higher than the earlier time points (*: p = 0.024, and **: p = 0.003).

**$\mu$-CT analysis**

The morphologies of new regenerated bone within the defects are shown in Fig. 27. In the early stage, it was found that new bone initially regenerated from the surrounding host bone and gradually increased its volume. Bone remodeling and its tendency to bridge defects was found in the later stage. The amounts of new bone regeneration over 8 weeks are demonstrated as new bone VF in table 4 and Fig. 28. It was found that the new bone VF of both groups increased with time. In contrast to the histological result, the new bone VF of group B was slightly greater than that of group A since week 4, but there was no significant difference (ANOVA, $p>0.05$).

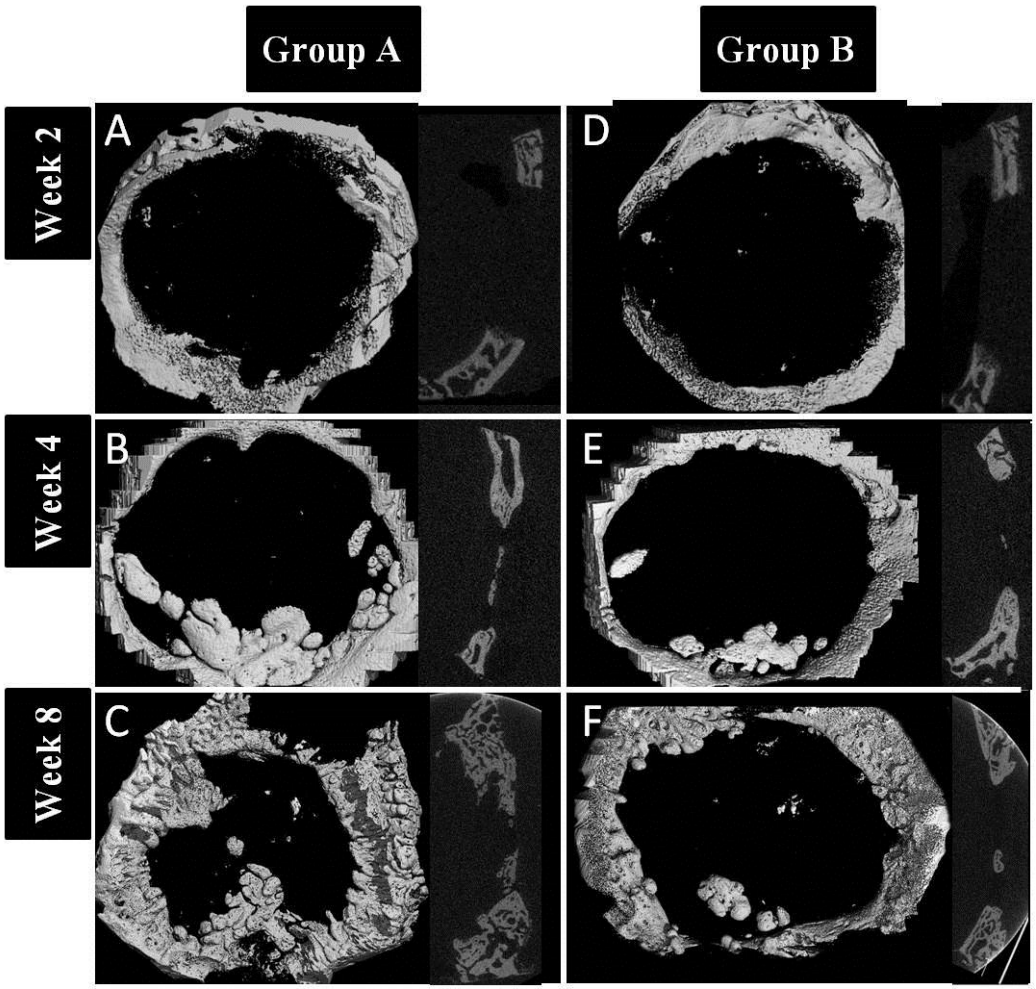


**Fig. 8** The 3-D reconstruction of the defects using $\mu$-CT over the observation periods are classified as group A: (A - C), group B: (D - F). In each image, the right side is coronal cut and the left side is axial cut.

**Table 3** The data of new bone VF for both groups over the observation periods.

| Study groups | New bone VF (%) (mean± SD) | | |
|---|---|---|---|
| | **2 weeks** | **4 weeks** | **8 weeks** |
| **Group A** | 6.962 ± 1.255 | 7.438 ± 3.577 | 9.982 ± 0.626 |
| **Group B** | 6.174 ± 2.393 | 8.202 ± 2.962 | 10.548 ± 2.494 |

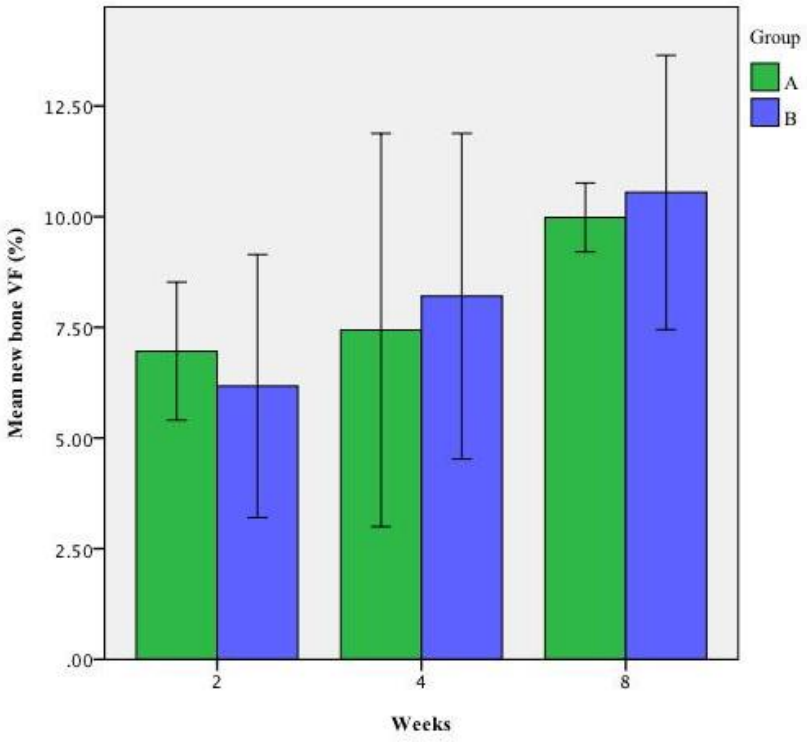


**Fig. 9** The graph demonstrates the average newly formed bone VF of both groups over 8 weeks. There was no statistical difference among the time points within group and between groups (ANOVA, $p>0.05$).

# Chapter 4

## Discussion

The study was performed mainly to discover the osteoconductive property of the PCL-CS 20% MSMD scaffold and the osteogenesis property of the bone cell-seeded scaffold by focusing on the volumes of new bone regeneration. Some protocols of the experiment were different from those of previous studies. Firstly, the 11-mm defects were smaller than the critical size defects of 15 mm in diameter by definition[74]. Several previous studies created their critical size defects in rabbit models in the range of 10-15 mm[75-79]. Recently, Sohn *et al*[79] created 15-mm and 11-mm defects in rabbits and they found that spontaneous new bone formation of both groups in 8 weeks were not significantly different. In our rabbit models, two 15-mm defects could not be created in each single cranium due to inadequate space. Therefore, two 11-mm defects were created instead in order to compare the efficacy of the two methods and reduce the errors between individual rabbits. Secondly, our observation period was shorter than those of previous similar studies, which ranged from 12 weeks to 9 months[49, 67, 68, 80, 81]. In our opinion, the duration of 8 weeks corresponds to the period of the bone remodeling process in humans and it was sufficient for estimating the efficacy for enhancing bone regeneration of the testing scaffolds. Finally, we combined the micro CT and the histomorphometric analysis in the same specimen for accurately assessing bone regeneration. In our opinion, the VF measured by the CT is the most accurate value for implying bone formation in 3-D. The AF measured by the histomorphometric analysis is less accurate for evaluating the total bone formation within the defects because the bone can be seen only along the directions of the tissue sections. However, the histomorphometric data is still the best method for demonstrating information of tissue responses to the scaffolds and maturity of the new bone. In addition, that data could reveal the areas of radiolucent PCL-CS scaffolds that could not be detected by the micro CT.

This study confirms that the PCL-CS MSMD scaffold is biocompatible and it can be implanted in vivo without complication. The histological sections demonstrated that new bone formation could regenerate from the host bone margins and gradually increased with time to consecutively occupy the defects. Remodeling of the new bone was detected since week 4. The profiles of the VF demonstrated that the average new bone regeneration enhanced by the cell-scaffold constructs was not different to that enhanced by of the scaffold alone. In addition, both of them could only gain a small amount of new bone into the defects. At week 8, the averages of new bone VF was 9.98 ± 0.63 % in group A and 10.55 ± 2.49% in group B. This result is similar to reports of some other studies[80-82]. Khojasteh, *et al*[82] mplanted the PCL-20%TCP scaffolds into 20 x 10 x 10 mm critical sized defects in dog's mandibles and found that the amount of new bone formation was 17.27 ± 3.29% after 8 weeks. Rai, *et al*[80] extended the observation period to 9 months for implantation of the same scaffolds into the 18 x 10 x 7 mm-mandibular defects of mongrel dogs. They also found that the minimum amount of new bone formation enhanced by the scaffold increased from 5.07± 2.13% to 9.78 ± 1.11% from 6 to 9 months. Similarly, Sawyer, *et al*[81] found that scaffolds alone gained less than 20% of new bone volume in a 5mm-rat calvarial critical-sized defect over 15 weeks.

Prior to seeding into the scaffolds, all of the autogenous bone marrow stromal cells harvested form the individual rabbit expressed their osteoblastic characters after induction. In addition, the SEM images prior to the implantation confirmed that those scaffolds could support attachment and proliferation of those cells very well. The histological results demonstrated that better vessel regeneration and less inflammatory cells were clearly found in the group of the cell-scaffold constructs compared to the group of the scaffolds alone. This phenomenon also related to the minimal necrotic zone in the inner portion of the cell-scaffold constructs. Nevertheless, neither the scaffolds alone nor in combination with the bone forming cells could enhance enough new bone regeneration for repairing bone defects in vivo. In addition, the histologic sections showed that there was no bone-scaffold integration and no morphologies of the cells detected on the surfaces of the scaffolds. It implies that those cells seeded into the scaffolds did not function to form new bone in vivo. The major possible reason is due to that

because the remarkable inflammatory cells induced by the scaffolds produced an unsuitable environment and interfered the functions of the cells. To find out whether this phenomenon was due to the property of the individual material of the scaffolds, some pure PCL MSMD scaffolds were implanted subcutaneously in rabbits to observe their tissue responses (data not shown). It was found that the PCL scaffolds induced minimum inflammatory response without the dominant cells including eosinophils and histeocytes, both of which responded to the PCL-CS scaffolds. This additional experiment showed the two important points. Firstly, using the MSMD technique concept can allow actions of the filler in the PCL-based scaffold directly affecting the surrounding cellular responses. Secondly, using CS as the filler of scaffolds seems to be inappropriate for repairing bone defects. Unlike the usual profile of chronic inflammatory reactions where neutrophil and lymphocyte are generally found, CS filler in our scaffolds attracted some specific cells including eosinophils and histeocytes. This corresponds with the reports of some studies that support correlation between chitosan and induction of some types of inflammatory cells[52, 83, 84]. Reese *et al*[85] reported that chitin as well as chitosan could induce tissue accumulation of IL-4-expressing innate immune cells, including eosinophils and basophils when given to mice. Barbosa *et al*[83] reported that the biological response to implanted chitosan scaffolds was influenced by the degree of acetylation (DA). They found that the DA 15% chitosan 3-D scaffolds induced a more intense inflammatory response when compared with DA 4% scaffolds. The DA 15% chitosan attracted high numbers of leukocytes and induced the formation of a thick fibrous capsule and a high infiltration of inflammatory cells within the scaffolds. They suggested that acetyl and amine functional groups of chitosan played an important role in that phenomenon. VandeVord *et al*[52] implanted porous chitosan scaffolds (DA 92%) in mice and found marked infiltration of neutrophils, which resolved with increasing implantation time. They suggested that unless some specific responses were caused by contaminating proteins from the source organism, those phenomenons were due to an inherent property of chitosan or its oligosaccharides that specifically interacted with neutrophil receptors. The authors concluded that although chitosan has a chemotactic effect on immune cells, this effect does not lead to a human immune response. Therefore, there were minimal signs of inflammatory reaction in the implanted sites and no evidence of infection or endotoxin was detected. That report was similar to the result

of our study where the PCL-CS scaffolds specifically induced some types of inflammatory cells without clinical signs of inflammation.

Regarding the results of this study, the concept of MSMD scaffolding is still valuable in terms of obtaining the active properties of the filler material and the proper architecture design. The interconnecting pore systems of the MSMD scaffolds can allow vessel regeneration throughout their inner portions which can increase healing of their surrounding tissue and survival of the grafts. In addition, the MSMD technique allows other materials that have stable properties within the range of 100-120$^{o}$C [32] to be combined with the PCL. Among those materials, bioactive biphasic calcium phosphate (HA:TCP), developed by our institute, is currently being experimented[86] and we plan to use this material as a filler in the future.

# Chapter 5

## Conclusion

Efficacy of the PCL-20%CS MSMD scaffolds combined with autogenous bone marrow stromal cells for repairing calvarial defects is not superior to that of the scaffold alone. However, combinations with those cells allow better neovascularization and reduce inflammatory reaction within the scaffolds. The study also indicated that the filler of the MSMD scaffolds can express its activity in animal models. However, chitosan seems to be an inappropriate filler for the PCL-based scaffolds for repairing bone defects in vivo in terms of inducing specific inflammatory reactions.

## Bibliography

1. Meyer U, Joos U, Wiesmann HP. Biological and biophysical principles in extracorporal bone tissue engineering. Part I. ***Int J Oral Maxillofac Surg.*** 2004;33:325-32.

2. Petite H, Viateau V, Bensaid W, Meunier A, de Pollak C, Bourguignon M, et al. Tissue-engineered bone regeneration. ***Nat Biotechnol.*** 2000;18:959-63.

3. El-Fayomy S, El-Shahad A, Omara M, Safe I. Healing of bone defects by guided bone regeneration (GBR): An experimental study. ***Egypt J Plast Reconstr Surg.*** 2003;27:159-66.

4. Roden RD, Jr. Principles of bone grafting. ***Oral Maxillofac Surg Clin North Am.*** 2010;22:295-300, v.

5. Deatherage J. Bone materials available for alveolar grafting. ***Oral Maxillofac Surg Clin North Am.*** 2010;22:347-52, v.

6. Kao ST, Scott DD. A review of bone substitutes. ***Oral Maxillofac Surg Clin North Am.*** 2007;19:513-21, vi.

7. Pryor LS, Gage E, Langevin CJ, Herrera F, Breithaupt AD, Gordon CR, et al. Review of Bone Substitutes. ***Craniomaxillofac Trauma Reconstr.*** 2009;2:151-60.

8. Nyan M, Sato D, Oda M, Machida T, Kobayashi H, Nakamura T, et al. Bone formation with the combination of simvastatin and calcium sulfate in critical-sized rat calvarial defect. ***J Pharmacol Sci.*** 2007;104:384-6.

9. Nkenke E, Schultze-Mosgau S, Radespiel-Troger M, Kloss F, Neukam FW. Morbidity of harvesting of chin grafts: a prospective study. ***Clin Oral Implants Res.*** 2001;12:495-502.

10. Precheur HV. Bone graft materials. ***Dent Clin North Am.*** 2007;51:729-46, viii.

11. Drosse I, Volkmer E, Capanna R, De Biase P, Mutschler W, Schieker M. Tissue engineering for bone defect healing: an update on a multi-component approach. ***Injury.*** 2008;39 Suppl 2:S9-20.

12. Boyce T, Edwards J, Scarborough N. Allograft bone. The influence of processing on safety and performance. ***Orthop Clin North Am.*** 1999;30:571-81.

13. Wiesmann HP, Joos U, Meyer U. Biological and biophysical principles in extracorporal bone tissue engineering. Part II. ***Int J Oral Maxillofac Surg.*** 2004;33:523-30.

14. Vacanti JP, Langer R. Tissue engineering: the design and fabrication of living replacement devices for surgical reconstruction and transplantation. ***Lancet.*** 1999;354 Suppl 1:SI32-4.

15. Rezwan K, Chen QZ, Blaker JJ, Boccaccini AR. Biodegradable and bioactive porous polymer/inorganic composite scaffolds for bone tissue engineering. ***Biomaterials.*** 2006;27:3413-31.

16. Engelberg I, Kohn J. Physico-mechanical properties of degradable polymers used in medical applications: a comparative study. ***Biomaterials.*** 1991;12:292-304.

17. Lei Y, Rai B, Ho KH, Teoh SH. In vitro degradation of novel bioactive polycaprolactone-20% tricalcium phosphate composite scaffolds for bone engineering. ***Mater Sci Eng C Mater Biol Appl.*** 2007;27:293-8.

18. Rai B, Teoh SH, Ho KH. An in vitro evaluation of PCL-TCP composites as delivery systems for platelet-rich plasma. ***J Control Release.*** 2005;107:330-42.

19. Schantz JT, Teoh SH, Lim TC, Endres M, Lam CX, Hutmacher DW. Repair of calvarial defects with customized tissue-engineered bone grafts I. Evaluation of osteogenesis in a three-dimensional culture system. ***Tissue Eng.*** 2003;9:S113-26.

20. Tay BY, Zhang SX, Myint MH, Ng FL, Chandrasekaran M, Tan LKA. Processing of polycaprolactone porous structure for scaffold development. ***jmatprotec.*** 2007;182:117-21.

21. Woodruff MA, Hutmacher DW. The return of a forgotten polymer-Polycaprolactone in the 21st century. ***J.Progpolymsci.*** 35:1217-56.

22. Ma J, Wang H, He B, Chen J. A preliminary in vitro study on the fabrication and tissue engineering applications of a novel chitosan bilayer material as a scaffold of human neofetal dermal fibroblasts. ***Biomaterials.*** 2001;22:331-6.

23. Sarasam A, Madihally SV. Characterization of chitosan-polycaprolactone blends for tissue engineering applications. ***Biomaterials.*** 2005;26:5500-8.

24. Shi C, Zhu Y, Ran X, Wang M, Su Y, Cheng T. Therapeutic potential of chitosan and its derivatives in regenerative medicine. ***J Surg Res.*** 2006;133:185-92.

25. Suphasiriroj W, Yotnuengnit P, Surarit R, Pichyangkura R. The fundamental parameters of chitosan in polymer scaffolds affecting osteoblasts (MC3T3-E1). ***J Mater Sci Mater Med.*** 2009;20:309-20.

26. Arpornmaeklong P, Suwatwirote N, Pripatnanont P, Oungbho K. Growth and differentiation of mouse osteoblasts on chitosan-collagen sponges. ***Int J Oral Maxillofac Surg.*** 2007;36:328-37.

27. Chupa JM, Foster AM, Sumner SR, Madihally SV, Matthew HW. Vascular cell responses to polysaccharide materials: in vitro and in vivo evaluations. ***Biomaterials.*** 2000;21:2315-22.

28. Jiang T, Abdel-Fattah WI, Laurencin CT. In vitro evaluation of chitosan/poly(lactic acid-glycolic acid) sintered microsphere scaffolds for bone tissue engineering. ***Biomaterials.*** 2006;27:4894-903.

29. Klokkevold PR, Vandemark L, Kenney EB, Bernard GW. Osteogenesis enhanced by chitosan (poly-N-acetyl glucosaminoglycan) in vitro. ***J Periodontol.*** 1996;67:1170-5.

30. Lahiji A, Sohrabi A, Hungerford DS, Frondoza CG. Chitosan supports the expression of extracellular matrix proteins in human osteoblasts and chondrocytes. ***J Biomed Mater Res.*** 2000;51:586-95.

31. Muzzarelli RA, Zucchini C, Ilari P, Pugnaloni A, Mattioli Belmonte M, Biagini G, et al. Osteoconductive properties of methylpyrrolidinone chitosan in an animal model. ***Biomaterials.*** 1993;14:925-9.

32. Thuaksuban N, Nuntanaranont T, Pattanachot W, Suttapreyasri S, Cheung LK. Biodegradable polycaprolactone-chitosan three-dimensional scaffolds fabricated by melt stretching and multilayer deposition for bone tissue engineering: assessment of the physical properties and cellular response. ***Biomed Mater.*** 2011;6:015009.

33. Thuaksuban N, Nuntanaranont T, Suttapreyasri S, Pattanachot W, Sutin K, Cheung LK. Biomechanical properties of novel biodegradable poly epsilon-caprolactone-chitosan scaffolds. ***J Investig Clin Dent.*** 1111;4:26-33.

34. Becker C, Jakse G. Stem cells for regeneration of urological structures. ***Eur Urol.*** 2007;51:1217-28.

35. Vacanti J. Tissue engineering and regenerative medicine: from first principles to state of the art. ***J Pediatr Surg.*** 2010;45:291-4.

36. Roberts SJ, Howard D, Buttery LD, Shakesheff KM. Clinical applications of musculoskeletal tissue engineering. ***Br Med Bull.*** 2008;86:7-22.

37. Kim SJ, Kim MR, Oh JS, Han I, Shin SW. Effects of polycaprolactone-tricalcium phosphate, recombinant human bone morphogenetic protein-2 and dog mesenchymal stem cells on bone formation: pilot study in dogs. ***Yonsei Med J.*** 2009;50:825-31.

38. Hutmacher DW. Scaffolds in tissue engineering bone and cartilage. ***Biomaterials.*** 2000;21:2529-43.

39. Salgado AJ, Coutinho OP, Reis RL. Bone tissue engineering: state of the art and future trends. ***Macromol Biosci.*** 2004;4:743-65.

40. Xiao X, Liu R, Huang Q, Ding X. Preparation and characterization of hydroxyapatite/polycaprolactone-chitosan composites.***J Mater Sci Mater Med.*** 2009;20:2375-83.

41. Yang X, Chen X, Wang H. Acceleration of osteogenic differentiation of preosteoblastic cells by chitosan containing nanofibrous scaffolds. ***Biomacromolecules.*** 2009;10:2772-8.

42. Jeong SI, Kim BS, Kang SW, Kwon JH, Lee YM, Kim SH, et al. In vivo biocompatibilty and degradation behavior of elastic poly(L-lactide-co-epsilon-caprolactone) scaffolds. ***Biomaterials.*** 2004;25:5939-46.

43. Yefang Z, Hutmacher DW, Varawan SL, Meng LT. Comparison of human alveolar osteoblasts cultured on polymer-ceramic composite scaffolds and tissue culture plates. ***Int J Oral Maxillofac Surg.*** 2007;36:137-45.

44. Mattanavee W, Suwantong O, Puthong S, Bunaprasert T, Hoven VP, Supaphol P. Immobilization of biomolecules on the surface of electrospun polycaprolactone fibrous scaffolds for tissue engineering. ***ACS Appl Mater Interfaces.*** 2009;1:1076-85.

45. Li Y, Danmark S, Edlund U, Finne-Wistrand A, He X, Norgard M, et al. Resveratrol-conjugated poly-epsilon-caprolactone facilitates in vitro mineralization and in vivo bone regeneration. ***Acta Biomater.*** 2011;7:751-8.

46. Piskin E, Isoglu IA, Bolgen N, Vargel I, Griffiths S, Cavusoglu T, et al. In vivo performance of simvastatin-loaded electrospun spiral-wound polycaprolactone scaffolds in reconstruction of cranial bone defects in the rat model. ***J Biomed Mater Res A.*** 2009;90:1137-51.

47. Huang JW, Chen WJ, Liao SK, Yang CY, Lin SS, Wu CC. Osteoblastic differentiation of rabbit mesenchymal stem cells loaded in A carrier system of Pluronic F127 and Interpore. ***Chang Gung Med J.*** 2006;29:363-72.

48. Yang F, Zhao SF, Zhang F, He FM, Yang GL. Simvastatin-loaded porous implant surfaces stimulate preosteoblasts differentiation: an in vitro study. ***Oral Surg Oral Med Oral Pathol Oral Radiol Endod.*** 2011;111:551-6.

49. Zhou Y, Chen F, Ho ST, Woodruff MA, Lim TM, Hutmacher DW. Combined marrow stromal cell-sheet techniques and high-strength biodegradable composite scaffolds for engineered functional bone grafts. ***Biomaterials.*** 2007;28:814-24.

50. Tarafder S, Nansen K, Bose S. Lovastatin release from polycaprolactone coated β-tricalcium phosphate: Effects of pH, concentration and drug–polymer interactions. ***Materials Science and Engineering: C.*** 2013;33:3121-8.

51. Venkatesan J, Kim SK. Chitosan composites for bone tissue engineering--an overview. ***Mar Drugs.***8:2252-66.

52. VandeVord PJ, Matthew HW, DeSilva SP, Mayton L, Wu B, Wooley PH. Evaluation of the biocompatibility of a chitosan scaffold in mice. ***J Biomed Mater Res.*** 2002;59:585-90.

53. Deans RJ, Moseley AB. Mesenchymal stem cells: biology and potential clinical uses. ***Exp Hematol.*** 2000;28:875-84.

54. Baddour JA, Sousounis K, Tsonis PA. Organ repair and regeneration: an overview. ***Birth Defects Res C Embryo Today.***96:1-29.

55. Li S, L'Heureux N, Elisseeff JH. Stem cell and tissue engineering. Singapore ; Hackensack, ***NJ: World Scientific***,; 2011. p. 1 online resource (xxiv, 448 p.).

56. Zhou YF, Sae-Lim V, Chou AM, Hutmacher DW, Lim TM. Does seeding density affect in vitro mineral nodules formation in novel composite scaffolds? ***J Biomed Mater Res A.*** 2006;78:183-93.

57. Bianco P, Robey PG, Simmons PJ. Mesenchymal stem cells: revisiting history, concepts, and assays. ***Cell stem cell.*** 2008;2:313-9.

58. Kagami H, Agata H, Tojo A. Bone marrow stromal cells (bone marrow-derived multipotent mesenchymal stromal cells) for bone tissue engineering: basic science to clinical translation. ***Int J Biochem Cell Biol.*** 2011;43:286-9.

59. D'Ippolito G, Schiller PC, Ricordi C, Roos BA, Howard GA. Age-related osteogenic potential of mesenchymal stromal stem cells from human vertebral bone marrow. ***J Bone Miner Res.*** 1999;14:1115-22.

60. Eslaminejad MB, Faghihi F. Mesenchymal Stem Cell-Based Bone Engineering for Bone Regeneration.

61. Pittenger MF, Mackay AM, Beck SC, Jaiswal RK, Douglas R, Mosca JD, et al. Multilineage potential of adult human mesenchymal stem cells. ***Science.*** 1999;284:143-7.

62. Griffin M, Iqbal SA, Bayat A. Exploring the application of mesenchymal stem cells in bone repair and regeneration. ***J Bone Joint Surg*** British volume. 2011;93:427-34.

63. Oliveira JM, Rodrigues MT, Silva SS, Malafaya PB, Gomes ME, Viegas CA, et al. Novel hydroxyapatite/chitosan bilayered scaffold for osteochondral tissue-engineering applications: Scaffold design and its performance when seeded with goat bone marrow stromal cells. ***Biomaterials.*** 2006;27:6123-37.

64. Sugiura F, Kitoh H, Ishiguro N. Osteogenic potential of rat mesenchymal stem cells after several passages. ***Biochem Biophys Res Commun.*** 2004;316:233-9.

65. Hildebrandt C, Buth H, Thielecke H. Influence of cell culture media conditions on the osteogenic differentiation of cord blood-derived mesenchymal stem cells. ***Ann Anat.*** 2009;191:23-32.

66. Agata H, Asahina I, Watanabe N, Ishii Y, Kubo N, Ohshima S, et al. Characteristic change and loss of in vivo osteogenic abilities of human bone marrow stromal cells during passage. ***Tissue engineering Part A.*** 2010;16:663-73.

67. Schantz JT, Hutmacher DW, Lam CX, Brinkmann M, Wong KM, Lim TC, et al. Repair of calvarial defects with customised tissue-engineered bone grafts II. Evaluation of cellular efficiency and efficacy in vivo. ***Tissue Eng.*** 2003;9 Suppl 1:S127-39.

68. Shao XX, Hutmacher DW, Ho ST, Goh JC, Lee EH. Evaluation of a hybrid scaffold/cell construct in repair of high-load-bearing osteochondral defects in rabbits. ***Biomaterials.*** 2006;27:1071-80.

69. Villalona GA, Udelsman B, Duncan DR, McGillicuddy E, Sawh-Martinez RF, Hibino N, et al. Cell-seeding techniques in vascular tissue engineering. ***Tissue Eng Part B*** Rev.16:341-50.

70. Wang Y, Uemura T, Dong J, Kojima H, Tanaka J, Tateishi T. Application of perfusion culture system improves in vitro and in vivo osteogenesis of bone marrow-derived osteoblastic cells in porous ceramic materials. ***Tissue Eng.*** 2003;9:1205-14.

71. Roh JD, Nelson GN, Udelsman BV, Brennan MP, Lockhart B, Fong PM, et al. Centrifugal seeding increases seeding efficiency and cellular distribution of bone marrow stromal cells in porous biodegradable scaffolds. ***Tissue Eng***. 2007;13:2743-9.

72. Toquet J, Rohanizadeh R, Guicheux J, Couillaud S, Passuti N, Daculsi G, et al. Osteogenic potential in vitro of human bone marrow cells cultured on macroporous biphasic calcium phosphate ceramic. ***J Mater Sci Mater Med.***1999;44:98-108.

73. Dominici M, Le Blanc K, Mueller I, Slaper-Cortenbach I, Marini F, Krause D, et al. Minimal criteria for defining multipotent mesenchymal stromal cells. The International Society for Cellular Therapy position statement. ***Cytotherapy.*** 2006;8:315-7.

74. Dodde R, 2nd, Yavuzer R, Bier UC, Alkadri A, Jackson IT. Spontaneous bone healing in the rabbit. ***J Craniofac Surg.*** 2000;11:346-9.

75. Pripatnanont P, Nuntanaranont T, Vongvatcharanon S. Proportion of deproteinized bovine bone and autogenous bone affects bone formation in the treatment of calvarial defects in rabbits. ***Int J Oral Maxillofac Surg.*** 2009;38:356-62.

76. Gosain AK, Santoro TD, Song LS, Capel CC, Sudhakar PV, Matloub HS. Osteogenesis in calvarial defects: contribution of the dura, the pericranium, and the surrounding bone in adult versus infant animals. ***Plast Reconstr Surg.*** 2003;112:515-27.

77. Shand JM, Heggie AA, Holmes AD, Holmes W. Allogeneic bone grafting of calvarial defects: an experimental study in the rabbit. ***Int J Oral Maxillofac Surg.*** 2002;31:525-31.

78. Nagata MJ, Melo LG, Messora MR, Bomfim SR, Fucini SE, Garcia VG, et al. Effect of platelet-rich plasma on bone healing of autogenous bone grafts in critical-size defects. ***J Clin Periodontol.*** 2009;36:775-83.

79. Sohn JY, Park JC, Um YJ, Jung UW, Kim CS, Cho KS, et al. Spontaneous healing capacity of rabbit cranial defects of various sizes. ***J Periodontal Implant Sci.*** 40:180-7.

80. Rai B, Ho KH, Lei Y, Si-Hoe KM, Jeremy Teo CM, Yacob KB, et al. Polycaprolactone-20% tricalcium phosphate scaffolds in combination with platelet-rich plasma for the treatment of critical-sized defects of the mandible: a pilot study. ***J Oral Maxillofac Surg.*** 2007;65:2195-205.

81. Sawyer AA, Song SJ, Susanto E, Chuan P, Lam CXF, Woodruff MA, et al. The stimulation of healing within a rat calvarial defect by mPCL Ì€“TCP/collagen scaffolds loaded with rhBMP-2. ***Biomaterials.*** 2009;30:2479-88.

82. Khojasteh A, Behnia H, Hosseini FS, Dehghan MM, Abbasnia P, Abbas FM. The effect of PCL-TCP scaffold loaded with mesenchymal stem cells on vertical bone augmentation in dog mandible: a preliminary report. ***J Biomed Mater Res B Appl Biomater.*** 101:848-54.

83. Barbosa JN, Amaral IF, Aguas AP, Barbosa MA. Evaluation of the effect of the degree of acetylation on the inflammatory response to 3D porous chitosan scaffolds. ***J Biomed Mater Res A.*** 1002;93:20-8.

84. Rucker M, Laschke MW, Junker D, Carvalho C, Schramm A, Mulhaupt R, et al. Angiogenic and inflammatory response to biodegradable scaffolds in dorsal skinfold chambers of mice. ***Biomaterials.*** 2006;27:5027-38.

85. Reese TA, Liang HE, Tager AM, Luster AD, Van Rooijen N, Voehringer D, et al. Chitin induces accumulation in tissue of innate immune cells associated with allergy. ***Nature.*** 2007;447:92-6.

86. Ebrahimi M, Pripatnanont P, Monmaturapoj N, Suttapreyasri S. Fabrication and characterization of novel nano hydroxyapatite/beta-tricalcium phosphate scaffolds in three different composition ratios. ***J Biomed Mater Res A.*** 1002;100:2260-8.

# Appendix

# Appendix

## Materials

### 1. Equipments and instruments

1.1 Autoclave, Tomy, High-pressure steam sterilizer ES-315, Tomy Seiko Co. LTD, Japan

1.2 Automatic pipette, Jencons™ Powerpipette Plus, Jencons Sciencetific Ltd., UK

1.3 Centrifuge, Eppendorf centrifuge 5417 C, Eppendorf AG, Germany

1.4 CO2 incubator, Thermo Forma series II, USA

1.5 Cryogenic mill, Freezer/Mill™ 6770, SPEX Sample Prep LLC, USA

1.6 Dry bath incubator, EL-02-220, MS major science, Taiwan

1.7 Inverted microscope, Nicon eclipse TS 100, Nicon instruments, Japan

1.8 Liquid nitrogen tank, Model HC-34 Liquid Dewar, Taylor-Wharton, USA

1.9 Microflow laminar downflow workstation, Astec Microflow Model ABS1200TCN, Bioquell Lab, UK

1.10 Micro-computed tomography, $\mu$CT35, Scanco Medical AG, Switzerland

1.11 Pipetter 100 - 1000 $\mu$L, Pipetteman Gilson™, France

1.12 Pipetter 20 - 200 $\mu$L, Pipetteman Gilson™, France

1.13 Pipetter 10 - 100 $\mu$L, Pipetteman Gilson™, France

1.14 Pipetter 2 - 20 $\mu$L, Pipetteman Gilson™, France

1.15 Refrigerated centrifugator, Hettich universal 320 R, Germany

1.16 Scanning electron microscope, JSM-5200, JEOL LTD, Japan

1.17 Slide-scanner, ScanScope, Aperio, USA

1.18 Sputter Coater, SPI-Module TM, Model 11425, SPI supplies, USA

1.19 Steriomicroscope, Nikon SMZ1500, Nikon instruments Inc., Japan

1.20 Testing sieve 75$\mu$m, Retsch GmbH, Germany

1.21 Universal testing machine, Lloyd, LRX plus, Lloyd instruments LTD, UK

1.22 Weight meter, Adventurer™, Electric balance Ohaus, Model AR2140, Ohaus Corp., USA

**2. Disposable materials**

2.1 Centrifuge tubes 50 ml, Cat. No. 373660, NUNC™, Denmark

2.2 Conical centrifuge tubes 15 ml, Cat. No. 366036, NUNC™, Denmark

2.3 Cryotube 1.8 ml internal thread, Cryotube™, Cat. No. 377267, NUNC™, Denmark

2.4 Microcentrifuge tubes 1.7 ml, Costar®, Cat. No. 3621, Corning Life Sciences, USA

2.5 Micropipette tips 1000 $\mu$L , Costar®, Cat. No. 4846, Corning Life Sciences, USA

2.5 Micropipette tips 1 - 200 $\mu$L , Costar®, Cat. No. 4845, Corning Life Sciences, USA

2.6 Micropipette tips 1 - 20 $\mu$L, Costar®, Cat. No. 4136, Corning Life Sciences, USA

2.7 Multidish 24-well plates, Nunclon Delta SI, Cat. No. 142475, NUNC™, Denmark

2.8 Multidish 48-well plates, Nunclon Delta SI, Cat. No. 150787, NUNC™, Denmark

2.9 Tissue culture flask 75 cm$^2$, Nunclon DSI, Cat. No. 156472, NUNC™ Brand product, Denmark

2.10 Tissue culture flask 25 cm$^2$, Nunclon DSI, Cat. No. 156346, NUNC™ Brand product, Denmark

**3. Chemical agents**

3.1 Absolute ethanol, Cat. No. 39420483, Merk, Germany

3.2 Acetone, Cat. No. 179973, Sigma-Aldrich™, USA

3.3 Alizarin red S, Cat. No. A5533-25G, Sigma-Aldrich™, USA

3.4 Alkaline phosphatase kit, AMP Buffer, IFCC, Human Diagnostics Worldwide, Germany

3.5 Beta-glycerolphosphate disodium salt hydrate 100g, Cat. No. G-9891, Sigma-Aldrich™, USA

3.6 Chitosan Middle-viscous, $\overline{M}_w$ $3 \times 10^5$–$5 \times 10^5$, 75–85% deacethylation, Cat. No. 28191, Fluka-Sigma-Aldrich™, Japan

3.7 Dexamethasone, Cat. No. D4902-25G, Sigma-Aldrich™, USA

3.8 Fetal Bovine Serum (FBS), Cat. No. 10270-106-500 ml, Gibco, Invitrogen™, USA

3.9 Fungisone/Amphothericin B, Cat. No. 15290-018-20 ml Gibco, Invitrogen™, USA

3.10 Glutaraldehyde solution 25% in $H_2O$ fror use as SEM fixative, Cat. No. G5882, Sigma-Aldrich™, USA

3.11 L-ascorbic acid, Cat. No. 79-500G, Unilab, Australia

3.12 Minimum essential medium alpha medium ($\alpha$-MEM) powder with L-glutamine, ribonucleosides, Cat. No. 11900-016, Gibco, USA

3.13 Penicillin 10,000 units/ml/Streptomucin 10,000 $\mu$g/ml, Cat. No. 15140-122-20 mg, Gibco, Invitrogen™, USA

3.14 Phosphate buffer saline 10X, Cat. No. 70013-073, Gibco, Invitrogen™, USA

3.15 Poly-epsilon-Caprolactone pellets 250 G, $\overline{M}_n$ 80,000 PC, Sigma Aldrich™, USA

3.16 Trypsin EDTA 0.5% 10x, Cat. No. 15400-54-100 ml, Gibco, Invitrogen™, USA

3.17 Trypan blue stain 0.4%, Cat. No. 15250-100 ml, Gibco, Invitrogen™, USA

3.18 Vinyl polysiloxane, 3M ESPE, USA

**4. Softwares**

4.1 EndNote X5 for Windows, Thomson Reuters, Philadelphia, USA

4.2 ImageScope, Aperio, USA

4.2 $\mu$CT 35 Version 4.1, SCANCO Medical AG, Switzerland

4.3 SPSS for Windows, version 14.0, SPAA Inc., USA

PRINCE OF SONGKLA UNIVERSITY
15 Karnjanawanij Road, Hat Yai, Songkhla 90110, Thailand
Tel (66-74) 286958 Fax (66-74) 286961
Website : www.psu.ac.th

MOE 0521.11/ 239 Ref.03/2014

March 6 , 2014

This is to certify that the research project entitled "The use of Polycaprolactone – Chitosan scaffolds combined with bone marrow stromal cells for repairing calvarial defects" which was conducted by Asst. Prof. Dr. Nuttawut Thuaksuban, Faculty of Dentistry, Prince of Songkla University, has been approved by The Animal Ethic Committee, Prince of Songkla University.

Kitja Sawangjaroen

Kitja Sawangjaroen, Ph.D.
Chairman,
The Animal Ethic Committee, Prince of Songkla University

ที่ ศธ 0521.11/ 236

สำนักวิจัยและพัฒนา
เลขที่ 15 ถนนกาญจนวนิช
มหาวิทยาลัยสงขลานครินทร์
อ.หาดใหญ่ จ.สงขลา 90110

Ref. 03/57

## หนังสือรับรอง

**โครงการวิจัย** การใช้โครงร่าง โพลีคาโปรแลคโตน-ไคโตซานร่วมกับเซลล์สร้างกระดูก เพื่อรักษารอยวิการของกะโหลกศีรษะ

**หัวหน้าโครงการ** ผศ. ดร.ทพ.ณัฐวุฒิ เทือกสุบรรณ

ได้ผ่านการพิจารณาและเห็นชอบจาก คณะกรรมการจรรยาบรรณการใช้สัตว์ทดลอง
มหาวิทยาลัยสงขลานครินทร์

ให้ไว้ ณ วันที่ 6 มีนาคม 2557

(ผู้ช่วยศาสตราจารย์ ดร.กิจจา สว่างเจริญ)
ประธานคณะกรรมการจรรยาบรรณการใช้สัตว์ทดลอง
มหาวิทยาลัยสงขลานครินทร์

iGRC2013
Global Issues and Awareness

**The Graduate School, Chiang Mai University**
**presents this certificate in confirmation that**

**VIVEK MANTALA**

**PRINCE OF SONGKLA UNIVERSITY**

**Participated in Presenting Research Results at**

**The International Graduate Research Congress (*i*GRC 2013)**

December 20, 2013

At The Empress Convention Center

The Empress Hotel, Chiang Mai, Thailand

**(Associate Professor Akachai Sang-in, Ph.D., DIC.)**

**Dean, the Graduate School**

**Chiang Mai University**

iGRC2013
Global Issues and Awareness

The Graduate School

50 CMU Anniversary

**The Graduate School, Chiang Mai University**
**This is to certify that**

**VIVEK MANTALA**
**PRINCE OF SONGKLA UNIVERSITY**

**has been awarded an Excellent Oral Presentation at**
**The International Graduate Research Congress (*i*GRC 2013)**

December 20, 2013
At The Empress Convention Center
The Empress Hotel, Chiang Mai, Thailand

**(Associate Professor Akachai Sang-in, Ph.D., DIC.)**
**Dean, the Graduate School**
**Chiang Mai University**

# Vitae

**Name** Vivek Mantala

**Student ID** 5510820026

**Education Attainment**

| Degree | Name of Institution | Year of Graduation |
|---|---|---|
| Doctor of Dental Surgery | Chiangmai University | 2009 |
| Higher Graduate Diploma in Clinical Science (Oral and Maxillofacial Surgery) | Prince of Songkla University | 2012 |

**Work-Position and address**

The Dental unit, ChiangKhum General Hospital, Chiangkhum, Phayao, Thailand, 56110

**Proceedings (Oral presentation)**

"The use of Polycaprolactone-Chitosan scaffolds combined with bone marrow stromal cells for repairing calvarial defects" in the 1st International Graduate Research Conference 2013 (iGRC 2013), 20 December 2013, Chiangmai, Thailand